X-ray to MR: the progress of flexible instruments for endovascular navigation

Progress in Biomedical Engineering

TOPICAL REVIEW

X-ray to MR: the progress of flexible instruments for endovascular navigation

Mohamed E M K Abdelaziz[1,*], **Libaihe Tian**[1], **Mohamad Hamady**[2], **Guang-Zhong Yang**[3] and **Burak Temelkuran**[1]

[1] The Hamlyn Centre for Robotic Surgery, Imperial College London, SW7 2AZ London, United Kingdom
[2] Department of Interventional Radiology, St Mary's Hospital, Imperial College Healthcare NHS Trust, W2 1NY London, United Kingdom
[3] Institute of Medical Robotics, Shanghai Jiao Tong University, Shanghai, People's Republic of China
[*] Author to whom any correspondence should be addressed.

E-mail: m.abdelaziz16@imperial.ac.uk

Keywords: cardiovascular diseases, endovascular interventions, x-ray fluoroscopy, magnetic resonance imaging, catheters, guidewires, robotics

OPEN ACCESS

RECEIVED
25 February 2021

REVISED
31 May 2021

ACCEPTED FOR PUBLICATION
9 July 2021

PUBLISHED
2 August 2021

Abstract

Interventional radiology and cardiology are rapidly growing areas of minimally invasive surgery, covering multiple diagnostic and interventional procedures. Treatment via endovascular techniques has become the go-to approach, thanks to its minimally invasive nature and its effectiveness in reducing hospitalisation and total time to recovery when compared to open surgery. Although x-ray fluoroscopy is currently the gold standard imaging technique for endovascular interventions, it presents occupational safety hazards to medical personnel and potential risks to patients, especially paediatric patients, because of its inherent ionising radiation. Magnetic resonance imaging (MRI), with its unique ability to provide radiation-free imaging, and acquiring morphologic and functional information, holds great promise in the advancement of image-guided navigation through the vasculature. Moreover, MRI has the potential to combine diagnosis, therapy and early evaluation of therapy in the same intervention. However, MR-guided interventions face a major challenge due to the presence of a large magnetic field (1.5/3 Tesla), which limits the set of materials suitable for the construction of key instrumentation (sheaths, catheters and guidewires). Despite these challenges, in recent years, significant progress has been made in the development of interventional devices, which comprise biocompatible, MR safe and MR visible materials. In an attempt to encourage and accelerate the development of MR-guided endovascular instrumentation, we present a systematic and illustrated overview of the plethora of work targeting to overcome the aforementioned limitations which are underpinned by the interdependent advancements in science, technology, engineering, mathematics and medicine (STEMM).

1. Introduction

Cardiovascular diseases (CVDs) are disorders and diseases affecting the heart or blood vessels, which lead to heart attacks, strokes, critical leg ischemia, and account for one-third of all deaths in the world (17.9 million annually) [1]. Endovascular interventions have become the backbone of treatment for CVDs thanks to the combined efforts of interventional radiologists, cardiologists, physicists, and engineers. These minimally invasive and image-guided procedures are carried out by manipulating thin, long, and relatively flexible instruments (sheaths, catheters, and guidewires) within the vasculature to gain access to specific blood vessels, commonly referred to as catheterisation. Subsequent to catheterisation, various treatment options such as angioplasty, stenting, embolisation and ablation, as illustrated in figure 1, are directed towards the diseased vessels. When compared to open surgery, these procedures not only lead to shorter convalescences, they also reduce operating time, hospitalisation, and total time to recovery.

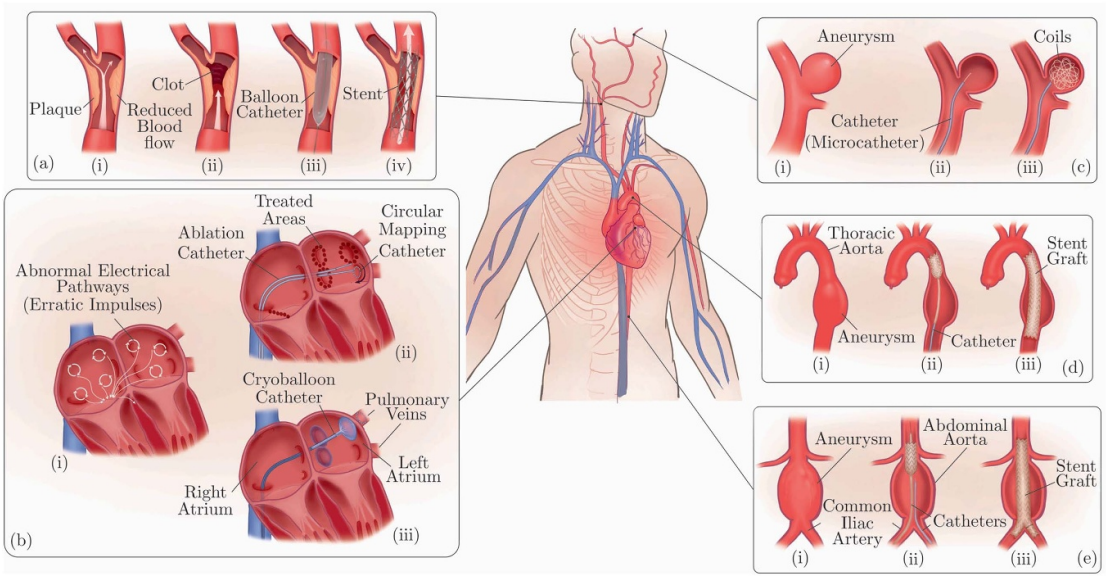

Figure 1. Cardiovascular diseases and their corresponding endovascular intervention(s): (a) Carotid arteries stenosis: narrowing of the arteries on either side of the neck which carry blood to the head, face and brain. This narrowing is usually the result of build-up of plaque within the arteries, a condition called atherosclerosis, Problems: (i) Reduced blood flow due to atherosclerosis plaque build-up, (ii) possible formation of clots caused by the irregular surface of the artery wall, Possible interventions: (iii) Carotid angioplasty: a catheter with a deflated balloon is threaded up into the carotid artery, and once it reaches the narrowed portion, the balloon is inflated (iv) Carotid stenting: after angioplasty, the balloon catheter is removed, and a self-expanding stent is placed over the plaque to hold open the artery. (b) Atrial fibrillation: irregular and often rapid heart rate, Problem: (i) Abnormal electrical pathways in the heart disrupt the heart's normal rhythm, Possible interventions: (ii) Radiofrequency (heat) catheter ablation of the pulmonary veins (PVs) to disrupt faulty electrical signals. A circular mapping catheter is used in parallel to map the electrical signals between the left atrium and the PVs, (iii) Cryoablation uses extreme cold instead of heat to restore regular heart rhythm. (c) Cerebral aneurysm: a bulged, weakened area of the cerebral artery wall, Problem: (i) Saccular aneurysm, Possible intervention: (ii) Endovascular Coiling: a catheter (microcatheter) is threaded up into the cerebral artery, (iii) A series of coils are pushed through the microcatheter. The coils fill the aneurysm which leads to clotting and protection from rupturing. (d) Thoracic aortic aneurysm: bulging of the aorta which extends from the chest to the abdomen, Problem: (i) Descending thoracic aortic aneurysm, Possible intervention: (ii) Thoracic endovascular aortic repair (TEVAR): a stent-graft deployment catheter is threaded into the aneurysm area, (iii) The stent-graft is deployed and helps maintain the blood flow through its lumens. (e) Abdominal aortic aneurysm: bulging of the lower part of the aorta (abdominal region), Problem: (i) Fusiform aneurysm, Possible intervention: (ii) and (iii) endovascular aneurysm repair (EVAR): similar to the TEVAR procedure d (ii) and d (iii).

X-ray fluoroscopy is currently the gold standard imaging technique for endovascular interventions. However, this imaging modality presents occupational safety hazards to medical personnel and potential risks to patients, especially paediatric patients, because of its inherent ionising radiation [2–5]. One of the contributing elements to increased radiation exposure is the use of fixed (pre-shaped) selective catheters and guidewires; designed for navigation through the vascular network. Despite its widespread use, selective catheters have limited manoeuvrability and as a result, are often associated with additional complications such as dissection, visceral and peripheral embolisation [6–8]. One way of improving manoeuvrability is to employ catheters with deflectable distal ends, i.e. steerable or deflectable catheters. Even though there have been significant advancements in catheter steering technologies targeting radiation dose reduction, there is a strong consensus among researchers and clinical staff that x-ray, with its perennial safety concerns, should be replaced by a safer alternative.

Magnetic resonance imaging (MRI) has revolutionised diagnostic medicine, allowing unparalleled visualisation of soft tissue [9]. It offers three-dimensional evaluations of pathology and function across the body. To benefit from the unique features of MRI, extensive research has been conducted in employing MRI as an alternative radiation-free imaging modality for image-guided procedures by combining diagnosis, therapy and early evaluation of the therapy in the same intervention [10–12]. However, for the transition to clinical practice, several challenges need to be addressed. Most notably, the lack of instruments well suited for MR-guided interventions [13, 14].

In this review, we first introduce commercial guidewires (section 2.1) and selective catheters (section 2.2), the current state-of-the-art devices used for navigational purposes in endovascular interventions. This introduction focuses on the structures, materials and manufacturing methods employed in the construction of these devices to provide background for the following sections. We then present their strengths and limitations in terms of navigation in the human vasculature and their accompanied side effects, mainly increased exposure to ionising radiation (section 2.3). This is followed by presenting one of

the proposed solutions to resolve their navigational shortcomings by introducing the concept of steerable catheters (section 2.3). We subsequently present a commonly proposed and investigated route, i.e. adopting MRI as an alternative imaging modality for its unique strength and capabilities when compared to x-ray fluoroscopy. To familiarise the reader with this imaging modality, we present the fundamental physics of MRI (section 3.1), followed by showcasing the ongoing efforts made by academia and industry to develop instruments compatible for use in MR environments through the adoption of different materials and manufacturing methods (sections 3.3–3.5). Lastly, we use our review as a base for defining the future requirements and challenges of developing MR safe and visible instrumentation for endovascular interventions (section 4). To generate this literature search, an up-to-date search (until October 2020) was carried out in databases such as PubMed, Science Direct, and patent databases (e.g. Espacenet). The keywords used here, which was greatly inspired by previous work [15–18], covered three main categories: (a) instrument (mr/mri/magnetic resonance (imaging), guide*, guidewire, steer*, deflect*, selective), (b) medical region (card*, heart*, atri*, vasc*), (c) instrument tracking (mr/mri/magnetic resonance (imaging), device tracking, catheter tracking, visualization).

2. Navigation under x-ray (fluoroscopy) guidance

2.1. Guidewires

Guidewires are a key tool used by interventional radiologists and cardiologists to navigate through the vasculature, allowing larger, less manoeuvrable devices (such as catheters) can be pushed over the wire to reach the targeted vessel rapidly. Commercial guidewires are available in different sizes, lengths and constructions (figures 2–4). The rich repertoire of guidewires is an excellent demonstration of the efforts going into the choice of materials and their smart processing, each having benefits helping interventionalists overcome different navigational challenges.

Guidewires, typically comprise of four major components: core wire, tip, body and coating [19, 20]. The central metallic core wire makes up most of the proximal section of the guidewire. The choice of core material(s) and its construction determines guidewire properties such as tip load, flexibility, steerability, trackability, torquability and support. Trackability is the ability of the guidewire's main body or shaft to follow its tip without buckling or kinking while navigating through the vasculature. Support, on the other hand, is the guidewire's ability to support the passage of other devices over it. Further, the thicker the core wire, the higher the support. Core wire materials are predominantly either stainless steel or nitinol. More recently, a combination of both materials is utilised to benefit from the columnar strength, pushability and torquability of stainless steel and the superelasticity and kink resistance of nitinol. In terms of construction, the core wire extends from the proximal end (shaft) of the guidewire and tapers towards the distal end to give the distal end more flexibility which facilitates guidewire navigation through tortuous anatomies. To achieve the desired taper profile across the distal end of the core wire (figure 2(b)), guidewire manufacturers commonly employ the process of centreless grinding. The longer the tapered section of the core wire, the better the guidewire trackability and the lower its tendency to prolapse. On the other hand, the shorter the tapering, the better the support property, at the price of an increased tendency to prolapse [19].

The tip refers to the relatively flexible distal end of the guidewire. Guidewire tips are classified based on the degree to which the tapered core wire extends to the dome-shaped, distal-most point of the guidewire. If the core wire is fused, welded or bonded directly to the distal-most point of the guidewire tip, then this is considered a core-to-tip design (figures 2(c), (d) and (f) and figures 3(a), (c), (e) and (g)). This design provides good tactile feedback and tip control with good torquability. Conversely, if the core wire is terminated several centimetres from the distal-most point and is replaced by a thin, flat stainless steel shaping or forming ribbon, then this is considered a shaping ribbon or forming ribbon design (figures 2(e), (g) and 3(b), (d), (f) and (h)). This design provides good shape retention and a unique softness and flexibility of the tip, at the cost of less tip torque control. Moreover, the guidewire tip also comprises a radiopaque element which is achieved either by adding a flexible radiopaque coil (e.g. platinum coil (figures 2(d)–(g)) coaxially to the core wire or by coating the tip of the core wire with radiopaque material (e.g. gold (figure 2(c))). Adopting radiopaque materials enhances the guidewire tip's visibility under fluoroscopy guidance. In several other embodiments, a secondary stainless steel or nitinol coil is placed coaxially (figures 3(a)–(d)) or in series (figures 3(e)–(h)) with respect to the aforementioned radiopaque coil to promote tip resilience, mechanical properties and tactile feedback. Instead of using secondary coils, other guidewire manufactures use diamond-cut nitinol hypotubes (figure 4(a)), by placing them coaxially to the radiopaque coil to enhance the guidewire's torquability and manoeuvrability (e.g. Fathom™ guidewire (Boston Scientific, MA, USA)).

The guidewire body refers to the additional encapsulation of material used to cover the core wire and distal coils(s). The material can either be in the form of a polymeric cover or a metallic spring coil (commonly stainless steel). In the case of polymeric covering, if the layer of polymer covers both the core wire and distal

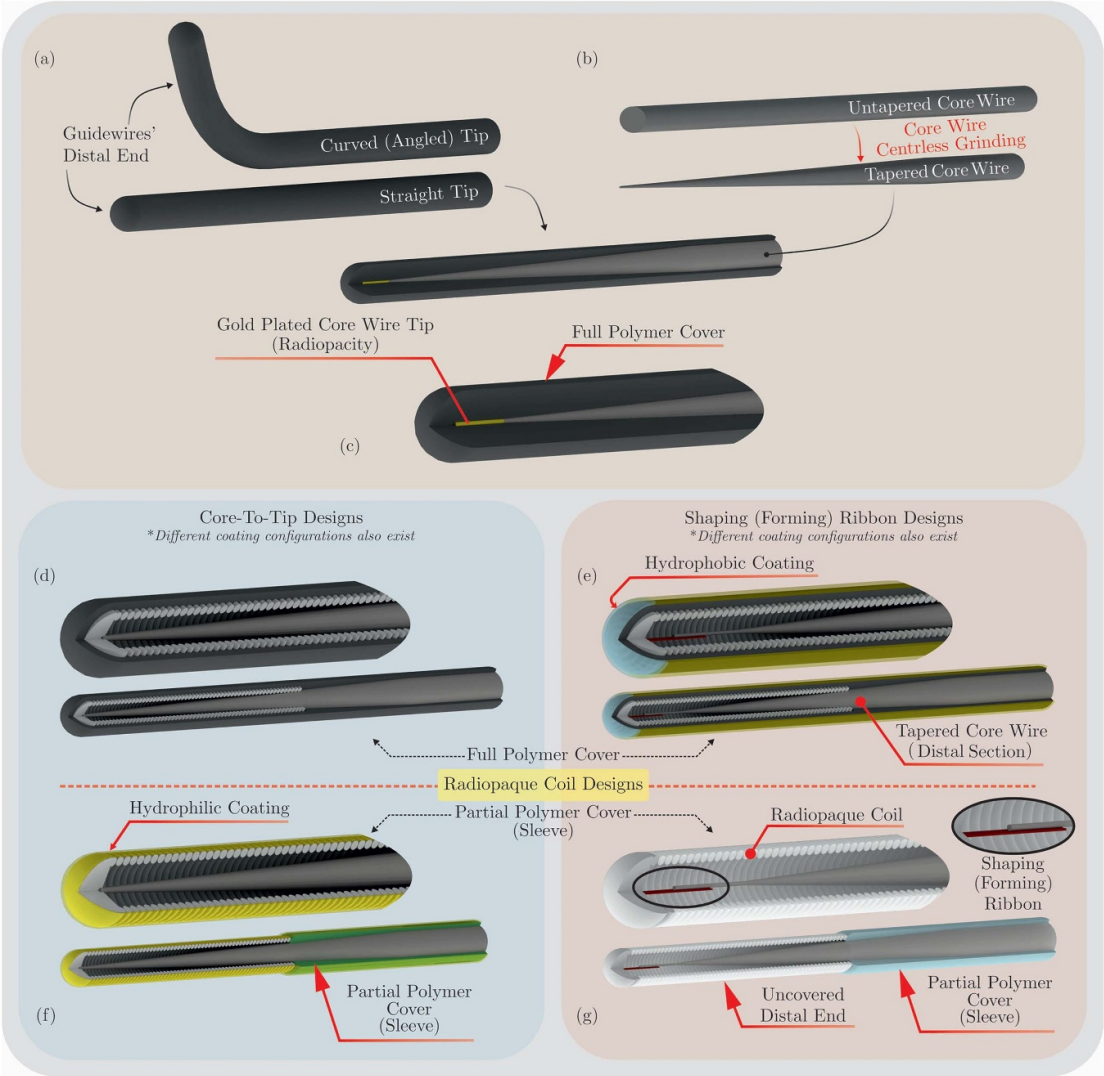

Figure 2. (a) Two different types of commonly used guidewire tips (distal ends): curved (angled) and straight. The distal ends tend to be heat treated to set the desired shape, e.g.'J'-shape [21]. (b) The transition from an untapered to a tapered core wire using centreless grinding to achieve the desired taper profile across the distal end in (c). For (c)–(g), a sectioned view of the distal end of commercially available guidewires and their corresponding insets, illustrating the core design and its surrounding elements (coils, ribbons, etc). (c) Guidewire widely used in peripheral interventions (Radifocus® Guidewire (Terumo Europe NV, Leuven Beligum)). This type has a core-to-tip design and is fully covered with polymer. For radiopacity, the tip is plated with a radiopaque material (gold in this illustration). (d)–(g) Guidewires comprising a radiopaque coil instead of the aforementioned radiopaque plated core tip. Classification based on **polymer covering**: (d) and (e) guidewires covered fully with polymer, and (f) and (g) guidewires partially covered with polymer. Classification based on **core design**: (d) and (f) core-to-tip design, and (e) and (g) shaping/forming ribbon design. Guidewire **coating**: (b) has an additional layer of hydrophilic polymer that is added to improve lubricity, trackability and manoeuvrability. On the other hand, (e) employs a hybrid approach by coating the distal-most point with a hydrophobic polymer (e.g. silicone) to enhance tactile feedback and tip control. Note: The illustrated examples are merely a few examples of commercially available coating configurations.

coil(s), then this is commonly referred to as a full polymer cover (figures 2(c)–(e) and figures 3(a), (b), (e) and (f)). This type of covering improves deliverability at the cost of losing tactile feedback. On the other hand, if the polymer covers only the proximal (untapered) section of the core wire, whilst keeping the distal coils and distal (tapered) section of the core wire uncovered, then this is considered a partial polymer cover, also referred to as sleeve or hybrid design (figures 2(f), (g) and 3(c), (d), (g) and (h)). This hybrid design not only improves tactile feedback, but it also ensures smooth deliverability. Other commercial guidewires (e.g. Amplatz guidewire), adopt the second type of covering, where a metallic spring coil covers the core wire and the radiopaque distal coils (if placed coaxially) alongside an additional safety flat wire (figures 4(b)–(d)). The safety wire in this design helps minimise the possibility of tip detachment if the spring coil breaks. Spring coil covered guidewires can be further classified into fixed core or movable core guidewires. As indicated by their names, for fixed core guidewires, the core wire cannot be moved with respect to the outer spring coil covering, conversely, the movable core guidewire allows the guidewire tip's softness and shape to be adjusted manually by moving the core wire back and forth with respect to the outer spring coil (figures 4(c) and (d)).

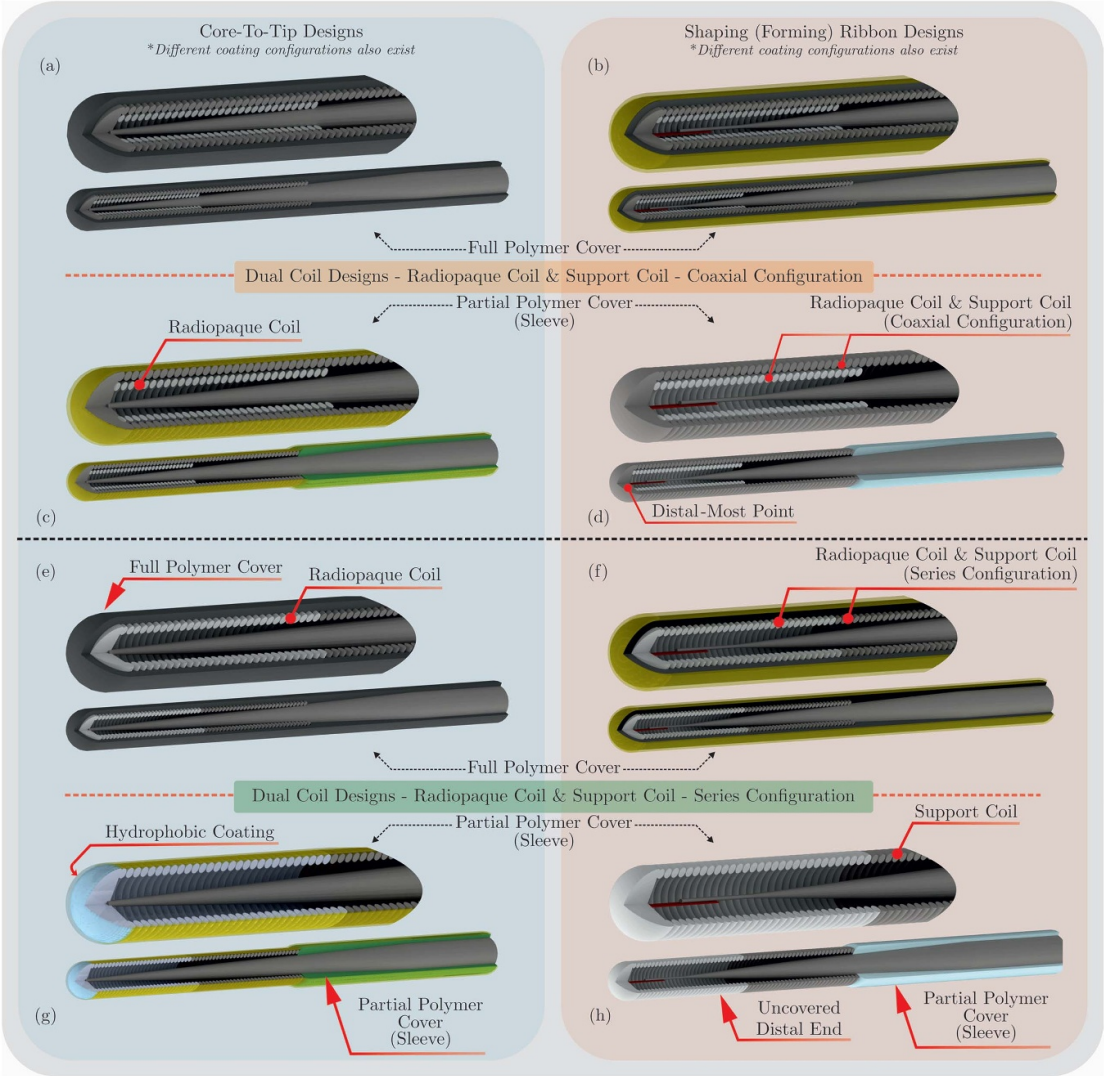

Figure 3. (a)–(h) Guidewires comprising a radiopaque coil and an additional support coil to promote the tip's resilience and mechanical properties. A sectioned view of the distal end of commercially available guidewires and their corresponding insets, illustrating the core design and its surrounding elements (coils, shaping ribbon). Classification based on **support coil placement**: (a)–(d) coaxially placed support coil (commonly stainless steel) with respect to a radiopaque coil, and (e)–(h) support coil placed in series with respect to a radiopaque coil. Classification based on **polymer covering**: (a), (b), (e) and (f) guidewires fully covered with polymer, and (c), (d), (g) and (h) guidewires partially covered with polymer. Classification based on **core design**: (a, c, e and (g) core-to-tip design, and (b), (d), (f) and (h) shaping/forming ribbon design. Guidewire **coating**: (b), (c) and (f) have an additional layer of hydrophilic polymer to improve the guidewires' lubricity, trackability and manoeuvrability. Conversely (g) employs a hybrid approach by applying a hydrophobic polymer (e.g. silicone) at the distal-most point to enhance tactile feedback and tip control. Note: The illustrated examples are merely a few examples of commercially available coating configurations.

In order to alleviate the surface friction and improve the guidewire's trackability and manoeuvrability, an additional layer of polymer coating (hydrophilic or hydrophobic) is added to the aforementioned elements. The hydrophilic coating's ability to attract water, makes the guidewire more lubricious and easier to navigate through tortuous anatomies. However in certain scenarios, the hydrophilically coated guidewire (figures 2(f), 3(b), (c) and (f)) can unintentionally end up in false subintimal spaces which increases the risk of perforation. Hydrophobic coating, on the other hand, enhances tactile feedback but decreases slipperiness and trackability. As shown in figures 2(e) and 3(g), hybrid coatings also exist, for instance, the dome-shaped distal-most point is coated with hydrophobic material for enhanced tactile feedback and tip control, while the distal coils or the entire guidewire as a whole is coated with hydrophilic material for smoother device delivery.

2.2. Selective catheters

A multitude of different catheters are developed for different tasks in image-guided endovascular interventions [6]. The catheters specifically designed for navigation in the vascular network, along with guidewires (figure 5), are called selective catheters. Most commercial selective catheters are passive, single

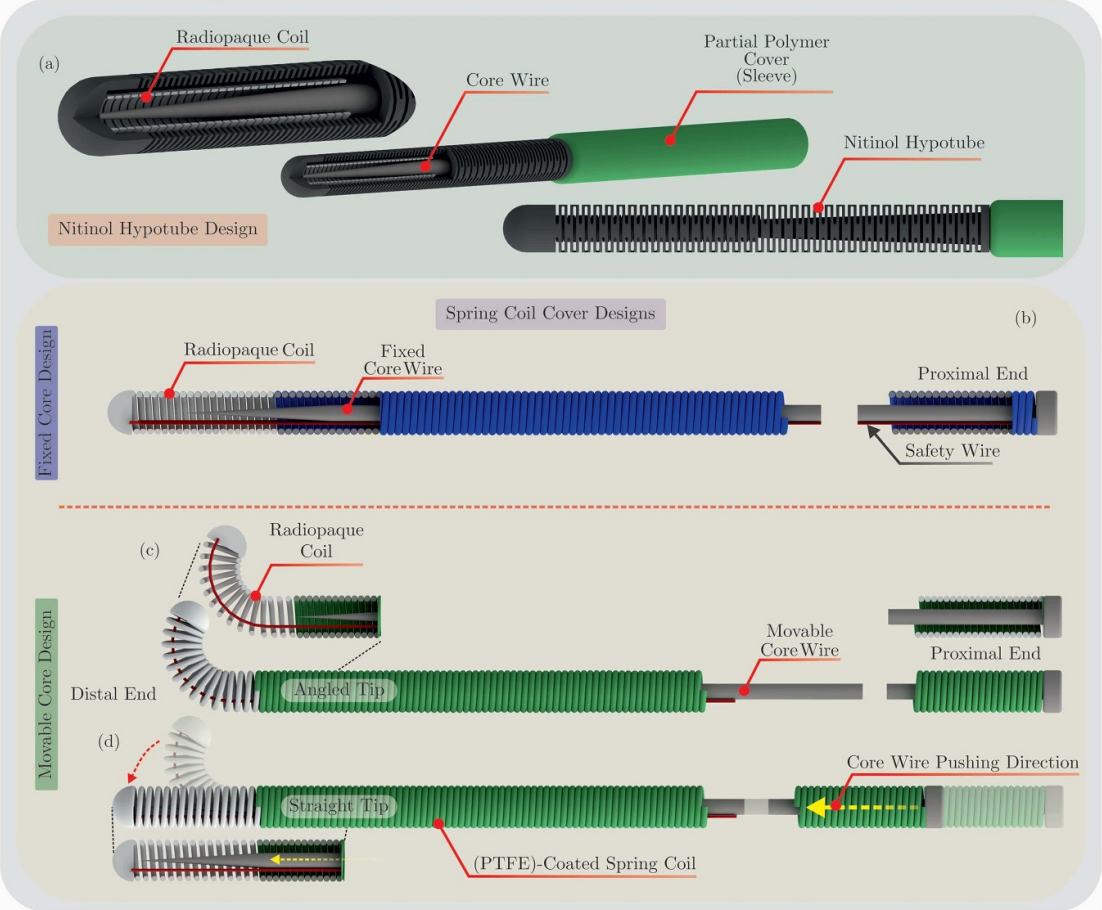

Figure 4. (a) A sectioned view of the distal end of a guidewire comprising a nitinol hypotube coaxially placed with respect to a radiopaque coil. The insets illustrate the core design and its surrounding elements (hypotube, core, coil). The design shown falls under the core-to-tip design category and consists of a partial polymer covering. Although not illustrated, the distal end can also be coated with hydrophilic/hydrophobic coatings to achieve the desired mechanical and physical properties. (b) Spring-coil covered guidewire with a fixed core design. (c), (d) Spring-coil covered guidewire with a movable core design. (c) Initial state of the guide wire, i.e. angled distal end (tip). (d) The proximal end is pushed, thereby moving the core wire with respect to the spring coil, which in turn straightens the distal end (tip). The safety wire in (b)–(d), illustrated in red, minimises the possibility of tip detachment if the spring coil breaks.

lumen tubing with pre-shaped distal ends mimicking the anatomy of blood vessels. They can be further classified into diagnostic angiographic catheters (DACs) and guiding catheters (GCs). DACs are used to inject a radiopaque contrast agent into cardiac, peripheral, or neurovascular blood vessels for angiography. Angiography is a medical imaging technique that uses real-time x-ray (fluoroscopy) to visualise blood vessels to help diagnose and evaluate diseases, such as aneurysms or atherosclerosis. Compared to DACs, GCs have larger inner lumens which facilitate the placement of other intravascular devices such as balloon and stent deployment catheters, into targeted blood vessels. Furthermore, GCs also permit contrast agent injection prior to angioplasty or stent deployment. In terms of construction, both types of catheters are typically comprised of a relatively stiff shaft and a soft pre-curved distal end with an atraumatic tip. The stiff shaft gives selective catheters enough pushability and torqueability to be inserted percutaneously into a peripheral blood vessel and to be navigated through the vasculature to a targeted site. Contrarily, the atraumatic tip minimises the risk of vessel perforation or dissection while manoeuvring the catheter through tortuous anatomies.

To achieve the desired stiffness and mechanical properties, catheter shafts are usually composed of metal braids sandwiched between layers of polymer; commonly polyurethanes, nylon 12, polyamide elastomers (e.g. PEBAX®) and fluoropolymers (e.g. polytetrafluoroethylene (PTFE)). In some cases, the polymers are blended with radiopaque fillers (e.g. barium sulphate—$BaSO_4$, bismuth subcarbonate—$(BiO)_2CO_3$) to increase the catheter's opacity to make them clearly visible under fluoroscopy. The metal braiding reduces the possibility of kinking or bending of the catheter during manipulation without a significant increase in the catheter's wall thickness. Thus, the same mechanical characteristics of thick-walled catheters can be achieved in thin-walled catheters [22]. Examples of metal braids include non-ferromagnetic metals such as 304 V, 304 L, and 316 L stainless steels; nickel-titanium (Nitinol); and tungsten for radiopacity [23]. To create

Table 1. Pros and cons of commercially available (x-ray fluoroscopy guided) guidewire configurations.

	Components		Configurations	Advantages and Disadvantages
X-ray Fluoroscopy Guided Guidewires	Core Wire	Material	Stainless steel	+ High columnar strength, pushability and torquability
			Nitinol	+ Superelasticity and kink-resistance
			Combination of stainless steel and nitinol	+ Benefits from both stainless steel and nitinol
		Tapered End	Long	+ Better trackability + Lower tendency to prolapse − Weaker support properties
			Short	+ Better support properties − Increased tendency to prolapse
	Tip	Tip Connection	Core-to-tip	+ Good tactile feedback + Tip control with good torquability
			Shaping (Forming) ribbon	+ Good shape retention + A unique softness and flexibility − Less torque control
		Radiopaque elements	Coating the tip of the core wire with radiopaque material	+ Highly flexible tip + One piece construction
			A flexible radiopaque coil placed coaxially to the core wire	+ Provides optimal XSS-ray visibility
			Secondary stainless steel or nitinol coil placed coaxially or in series	+ Promotes tip resilience + Better mechanical properties + Better tactile feedback
			Diamond-cut nitinol hypotubes placed coaxially to the radiopaque coil	+ Enhanced torquability and maneuverability
	Body	Polymeric Cover	Full polymer cover	+ Better deliverability − Decreased tactile feedback
			Partial polymer cover	+ Improved tactile feedback + Smooth deliverability
		Metallic Coil	Fixed core	+ Provides good support properties and stability
			Movable core	+ Adjustable tip softness and shape
	Coating	Hydrophilic		+ More lubricious + Easier to navigate through tortuous anatomies − Risk of unintentionally ending up in false subintimal spaces
		Hydrophobic		+ Enhanced tactile feedback − Decreased slipperiness and trackability
		Hybrid (hydrophobic distal point and hydrophilic shaft)		+ Enhanced feedback and tip control + Smoother device delivery

flexible distal ends, catheter manufacturers employ a plethora of techniques. One common approach is to thermally bond a relatively flexible tubing to the relatively stiff composite laminated catheter shaft. Other techniques include varying the braid pitch of the reinforcement metal braid or varying the hardness of materials used in constructing the outer layer. Once fabricated, the resulting catheter may be coated with hydrophilic, lubricious polymers such as silicone and poly(vinylpyrrolidone) (PVP) to reduce frictional forces and risk of damage to blood vessel walls [24].

In terms of differences, DACs have smaller inner lumens and tapered distal tips. Tapered distal tips maximise flexibility and facilitate navigation through tight and tortuous anatomies [27]. GCs, on the other hand, have larger inner lumens and un-tapered distal tips. Most commercial GCs follow a two-layer catheter assembly with a chemically etched PTFE liner as an inner layer, braided stainless steel wires for reinforcement and multi-durometer PEBAX® as an outer layer. The PTFE liner's outer layer is etched to enhance its bondability with the PEBAX® outer layer. PTFE is frequently used as an inner layer because of its low coefficient of friction (0.05–0.8, static) which facilitates the insertion of other devices through GCs [28]. Similarly, PEBAX®, is widely used in the manufacturing of catheters because of its extensive range of hardness and flexibility, and superior bonding capability with other polymers [29]. Figure 6 illustrates the fabrication steps of commercial GCs [30].

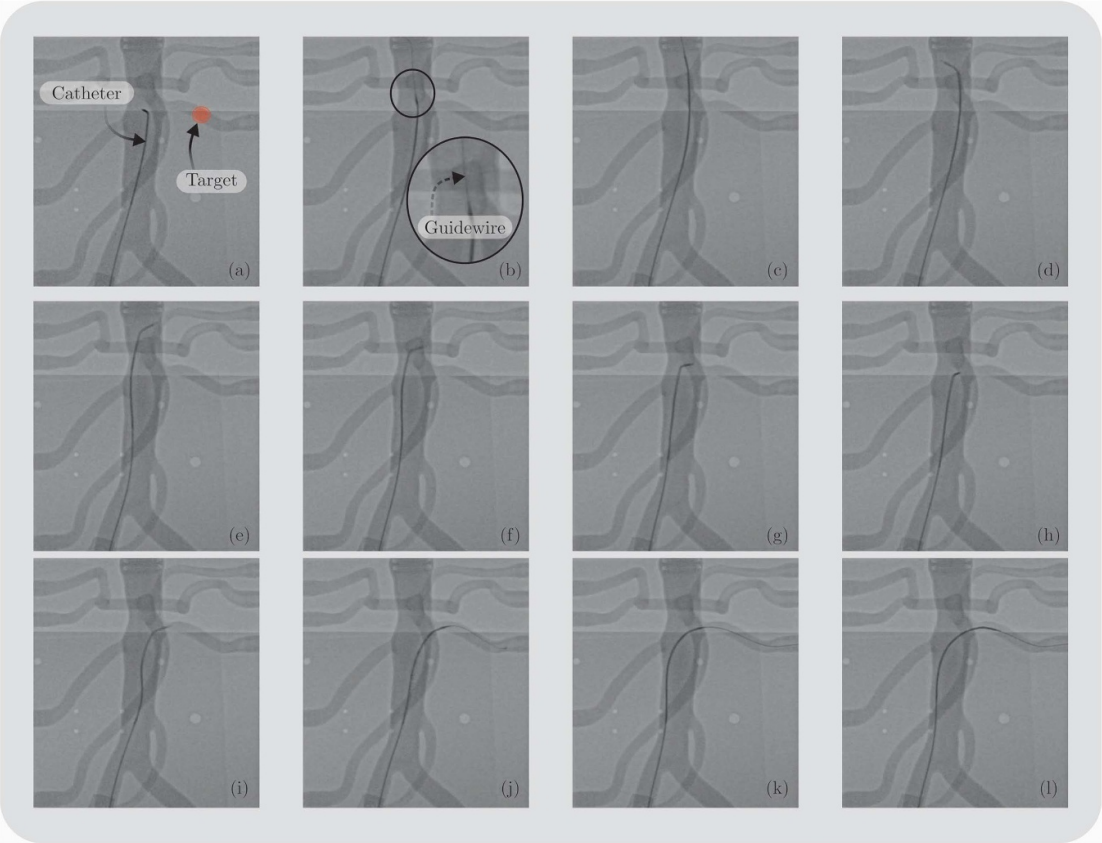

Figure 5. 2D x-ray fluoroscopy sequence illustrating the catheterisation of the left renal artery (LRA) in an abdominal phantom (Elastrat, Geneva, Switzerland) using a selective catheter, IMPRESS®, size = 5 F (1.667 mm outer diameter), distal end shape: headhunter 1, length = 100 cm, inner diameter = 0.046″ (1.17 mm), Reference: 510035HH1 (Merit Medical OEM, UT, US) and a guidewire, Radifocus® Guidewire M Standard Type Guidewire, length = 180 cm, Outer Diameter = 0.035″, flexible length = 10 mm, Angled Distal Tip, Reference: RF-GA35181M, (Terumo Europe NV, Leuven Beligum). (1) Indicates the LRA target and the catheter. (2) Guidewire is advanced over the LRA whilst keeping the catheter in place. The catheter's distal end straightens due to the advancement of the guidewire. (3) Catheter is advanced over the guidewire. (4) Guidewire is partially retracted and the catheter restores the pre-shaped distal end. (5) The catheter is rotated to adjust its orientation. (6)–(8) The catheter and guidewire assembly is slowly retracted towards the LRA. (9) The catheter's distal end slides into the LRA, (10)–(11) The guidewire is advanced through the catheter to prevent the catheter from flipping back to the abdominal aorta. (12) The catheter is advanced over the guidewire.

2.3. Challenges associated with navigation under x-ray (fluoroscopy guidance)

One of the critical challenges clinicians face while preparing for an intervention is choosing the appropriate selective catheters and guidewires from the myriad of shapes, sizes, and features (stiffness, braiding, coating) [6]. Furthermore, steering and manoeuvring of selective catheters and guidewires can become complicated due to their fixed shape at the distal end, long lengths, and unpredictable friction between the devices and vessel walls. In specific scenarios, where multiple catheterisations are performed, e.g. Fenestrated Endovascular Aortic Aneurysm Repair (FEVAR), interventionalists exchange catheters to change the tip shape and guidewires to change its stiffness. The navigation difficulties and repeated instrument exchange consequently increase the risks of complications, such as infection, distal embolisation, dissection, perforation of vessels, and increase procedure time. Since endovascular interventions are performed under x-ray fluoroscopy guidance, any difficulty in navigation increases the exposure of patient and staff to ionising x-ray radiation. Besides, using x-ray fluoroscopy as an imaging modality per se introduces other drawbacks which make it sub-optimal for image-guided endovascular interventions. X-ray poorly depicts soft tissue contrast [31], may lead to significant career musculoskeletal injury to operators forced to wear protective lead aprons (designed to shield the body from harmful radiation) [32], increases cancer risks for paediatric patients who undergo cardiac catheterisation procedures [33], and may impair kidney function due to the use of large volumes of iodine-containing contrast media (used to visualise the blood vessels in fluoroscopy-based angiography) [34].

A commonly proposed technique to overcome the aforementioned navigational challenges is to use robotic platforms (summarised in the following sections 2.4.1–2.4.3) to remotely and accurately manipulate off-the-shelf passive instrumentation (selective catheters, guidewires) and steerable catheters. Steerable

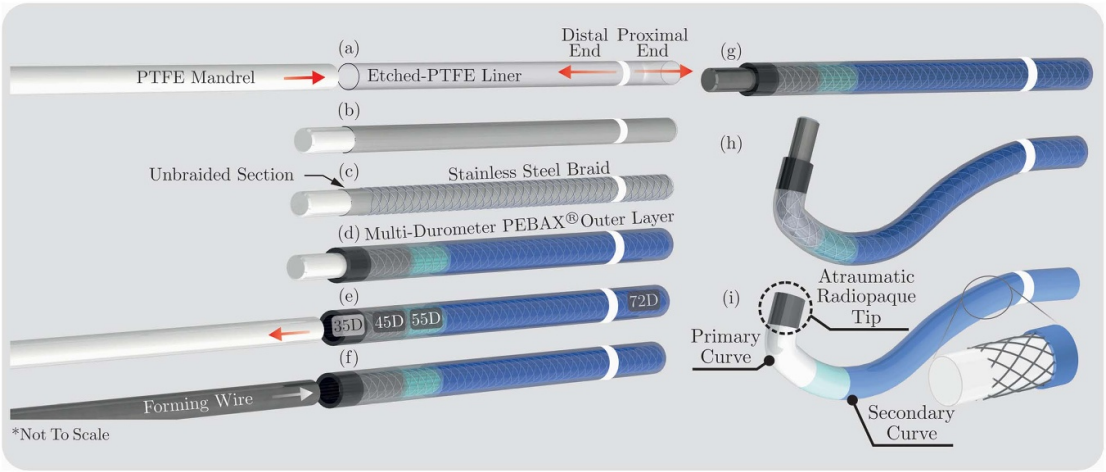

Figure 6. Guiding catheter fabrication steps: (a) a ram extruded PTFE mandrel is fed through a chemically etched ram extruded PTFE liner to prevent the liner from collapsing during the subsequent processes. (b) The liner/mandrel assembly is then braided with stainless-steel wires (e.g. 50 μm 316 L stainless-steel round wires) using a maypole braiding machine. (c) A small section of the liner is left non-braided to create a flexible atraumatic tip. (d) A multi-durometer PEBAX® outer layer is applied on top of the braided liner/mandrel assembly to encapsulate the braid. The stiffness of the outer catheter decreases progressively from the proximal end (Shore Hardness 72D) to the distal atraumatic radiopaque tip (Shore Hardness 35D). The transition segments (45D and 55D) are added to reduce the possibility of catheter kinking caused by abrupt changes in flexibility. This fabrication step can be achieved using various techniques, including thermal bonding of multi-durometer segments [25], intermittent extrusion [26]. (e) The PTFE mandrel is pulled out of the laminated tube. (f)–(g) The laminate is mounted onto a forming wire to form the desired distal end shape. (h) The distal end shape is modified using a template (e.g. Judkins right 4) and placed in a forming oven for a predetermined temperature and time. (i) After annealing, the assembly is cooled, followed by the removal of the forming wire.

catheters are catheters with improved manoeuvrability and stability, integrated with an actuation mechanism which enables the operator to change the distal end shape of the catheter manually or remotely (robotically). Commercial and under development steerable catheters make use of four actuation mechanisms: tendon-driven (also referred to as pull-wire driven or cable driven), magnetic, smart material-actuated and hydraulic [15]. Tendon-driven steerable catheters are the largest and most clinically used group of steerable catheters, especially in the field of cardiac electrophysiology. In addition to navigating through tortuous anatomies and guiding other intravascular devices, tendon-driven catheters embedded with conductive wires are used in the treatment of cardiac arrhythmia, i.e. abnormal heart rhythms (figure 1(b)). Other applications include catheter-based intra-cardiac echocardiography (ICE), which is used in the visualisation of cardiac structures and blood flow. Apart from tendon-driven catheters, steering and orienting of catheters via controlled magnetic fields is one of the few robotic technologies that are commercially available, e.g. Niobe® and Genesis RMN® magnetic systems (Stereotaxis, Saint Louis, MO, USA). As in the case of tendon-driven catheters, the aforementioned magnetic systems are employed in cardiac electrophysiology [35]. To the best of our knowledge, the other two steering mechanisms (smart material-actuated and hydraulic) are yet to be used in an operating theatre. The different configurations of steerable catheters will be presented in section 3.4.

2.4. Robot-assisted platforms for endovascular interventions

Recent advancements in robotic catheterisation systems aim to help surgeons manipulate instrumentation more effectively in order to improve surgical outcomes and to minimise radiation exposure for both the patients and clinicians alike. Robotic platforms can also eliminate hand tremors of the operator, and improve the stability and precision of procedures [36]. Furthermore, the adoption of remote manipulation allows the operator to perform the procedure with added comforts, without heavy protection suits [37]. Several commercial platforms have been developed for peripheral vascular interventions and electrophysiology.

2.4.1. Commercial platforms for general vasculature (PVI, PCI)

Peripheral vascular interventions (PVI) are minimally invasive procedures used to treat diseases in the arteries leading to the intestines, head, arms and most commonly the legs. Percutaneous coronary interventions (PCI) on the other hand, treat diseased vessels in the heart. For fluoroscopy-guided peripheral vascular interventions, the discontinued Magellan™ robotic platform (Johnson & Johnson, Redwood City, CA, USA) was designed to allow clinicians to remotely manipulate proprietary pull-wire driven steerable catheters/sheaths and standard off-the-shelf guidewires through a variety of anatomies and lesions from a remote workstation. Each bespoke steerable device comprised a base at its proximal end, which facilitated its

coupling into a motorised actuation unit. The base of each instrument consisted of spring-loaded idler pulleys through which the pull-wires were routed and anchored. The rotation of the pulleys led to the tensioning and loosening of the pull-wires, which subsequently deflects the device's flexible distal end. Besides, the actuation unit enabled the precise advancement and retraction of the device. Similarly, it was also possible to translate and rotate guidewires by placing them between two conveyor belts which mimicked the surgeons' manipulation of guidewires using their thumb and forefinger. To manipulate the instruments, surgeons used a 3D joystick or navigation buttons which were located on the workstation. The Magellan™ robotic system was successfully used in several peripheral arterial interventions such as stent grafting and aneurysm repair [38, 39]. The limitations of the Magellan™ platform included its high installation costs and use of non-standard catheters and sheaths. Furthermore, the system did not allow the integration of therapeutic devices, which limited its use for navigation purposes only.

A recent trend in commercial robotic platforms, e.g. CorPath GRX® (Siemens Healthineers, Waltham, MA, USA), facilitate the use of standard off-the-shelf devices. The CorPath GRX® system is the only commercially available FDA approved and CE-marked robotic platform dedicated for endovascular peripheral and coronary interventions. The GRX® platform builds upon its predecessor, the CorPath 200® [40], by enabling the control of a selective guiding catheter, along with a guidewire and a therapeutic catheter (e.g. balloon/stent). To dock the guiding catheter into the platform, the proximal luer lock of the guide catheter is connected to a drive gear add-on. The assembly is then mounted onto an actuation unit which enables the translation and rotation of the guiding catheter respectively. The guidewire and therapeutic catheters, on the other hand, are loaded into the robotic platform by placing them between a set of active and passive rollers (also referred to as friction wheels) which facilitate the insertion/retraction and rotation of the instruments. Similar to the Magellan™, the clinician remotely manipulates the instruments in a shielded cockpit using joystick and touchscreen controls. The GRX® platform includes other features such as partial automation (Rotate on Retract feature) [41], and long distance teleoperation (20 miles away from the patients) [42]. Another emerging robotic platform dedicated for PCI procedures is the R-one™ system (Robocath, Rouen, France). The platform features a robotic manipulator for off-the-shelf guidewires and balloon catheters. The system recently obtained its CE certification. Other platforms that are currently under development include: (1) Endoways platform (Endoways, Or Yehuda, Israel), (2) Coral (Moray Medical, CA, USA), (3) WeMed's platform (WeMed, Beijing, People's Republic of China), (4) Shanghai Aopeng Medical's platform (Shanghai Aopeng Medical Technology Co. Ltd, Shanghai, People's Republic of China).

2.4.2. Commercial platforms for electrophysiology (EP)

Electrophysiology (EP) is the diagnosis and treatment of patients with electrical or rhythm disorders of the heart. Sensei® X2 by Hansen Medical (Johnson & Johnson, Redwood City, CA, USA) was a major commercial robotic platform dedicated for cardiac electrophysiology therapies [43, 44]. Similar to the Magellan™, the Sensei® platform comprised two pull-wire driven steerable catheters/sheaths, one inside the other. The inner guide catheter is flexible and accommodates standard ablation catheters while the outer guide sheath provides stability. The system also follows a master-slave architecture, where the operator remotely controls the instrumentation using a 3D joystick or navigation buttons. Unlike the Sensei® system, the Amigo™ Remote Catheter System (RCS) (Catheter Precision In, Mount Olive, NJ, USA) platform is a catheterisation system that navigates third party standard EP mapping and ablation steerable pull-wire driven catheters [45–49]. The system is equipped with an intuitive remote controller that replicates the manual handle of a steerable catheter. Wutzler *et al* reported that the use of the Amigo™ RCS for the treatment of atrial fibrillation led to a significant reduction in fluoroscopy exposure for the operator when compared to manual interventions (13.4±6.1 vs. 23.9±5.4 min, $p < 0.001$) [50].

Another commercially available platform which employs magnetic steering is the Niobe® (Stereotaxis, Saint Louis, MO, USA) system. The robotic system consists of two large permanent magnets located on either side of the patient's bed. The rotation of the magnets using motors results in the subsequent steering of a steerable catheter embedded with a magnet at its distal end. As reported by Stereotaxis, the robotic platform has been already used in more than 100 000 procedures, and has been validated by several research groups through *in-vivo* and clinical trials in the treatment of cardiac arrhythmia [51–61]. The Genesis RMN® magnetic system is the more recent upgraded successor of the Niobe®. The platform is smaller in size, lighter, faster and more flexible when compared to the Niobe® platform. The aforementioned benefits result in improved responsiveness of the magnetic steering system and patient access for medical personnel (nursing team and anaesthetists). Stereotaxis has also commercialised a robotic navigation system (Vdrive) to remotely control third party diagnostic pull-wire driven steerable catheters. The Vdrive system consists of components such as the V-Sono™ manipulator. This manipulator controls ICE steerable catheters such as the SoundStar® (Johnson & Johnson, Redwood City, CA, USA) or Siemens AcuNav™ (Siemens Healthineers, Waltham, MA, USA).

Catheter Guidance Control and Imaging (CGCI) system (Magnetecs Corporation, CA, USA) is another master-slave, magnetic-based catheter navigation system which uses eight electromagnets, four of which are placed in a semi-spherical arrangement above the patient's bed, and the other four are placed symmetrically underneath the patient's torso [62–64].

The eight electromagnets generate a 'lobed' shaped dynamic magnetic field within the region of the patient's heart. Controlling the magnitude, direction and gradient of the generated magnetic fields results in the formation of a force or torque applied on a steerable catheter equipped with magnets at its distal tip. Another magnetic catheter steering system that employed seven electromagnets around the patient's torso for the treatment of cardiac arrhythmia is the Aeon Phocus system (Aeon Scientific AG, Zurich, Switzerland). As in the case of the Niobe® and CGCI systems, the operator can remotely control a steerable magnetic catheter with a joystick in a separate control room. Although the system was CE marked in 2014, Aeon Scientific is no longer in business. The main limitation of the aforementioned magnetic-based systems is the need for large magnets which usually require special considerations for operating theatres.

2.4.3. Emerging research platforms for endovascular interventions

A variety of robotic systems for endovascular interventions were reported in literature. In general, such systems show low levels of robotic autonomy [65] and consider a master-slave set-up for teleoperated manipulation of instrumentation. Feeding (advancing and retracting) of catheters and guidewires are normally achieved by roller-based mechanisms [66–72] or linear drives integrated with electromechanical clamps [73]. The corresponding master, with human machine interfaces (HMIs), make use of conventional stationary joysticks, hand-held joysticks, or 3D input devices with force feedback capabilities. Novel master devices were proposed to improve the transparency of teleoperation. Exemplary, motion due to manipulation of standard catheters was sensed without user feedback and replicated to a slave robot [74]. More recently, magnetorheological fluid was used in combination with a catheter to mimic friction and generate user feedback [75]. Slave robots generally show alternative concepts with different electro-mechanical mechanisms for driving and clamping of instrumentation as reported in [76–78]. Device compliance with MR environments is restricted to [79–82], where researchers substitute covnentional electric motors with non-ferromagnetic ultrasonic motors [79], hydraulic motors [80], and pneumatic stepper motors [81, 82]. For the sake of completeness, the reader is kindly referred to other comprehensive reviews of the emerging platforms [36, 83, 84].

3. Navigation under MR guidance

3.1. MRI and MR-guided endovascular interventions

Although the usage of steerable sheaths/catheters and robotic systems contribute to improved stability and procedural efficacy [85–88], recent developments in cardiovascular science have highlighted the importance of including functional information (e.g. blood flow, tissue oxygenation, diffusion, perfusion) of the underlying pathology during endovascular interventions to guide treatment/therapy decisions [89]. Magnetic resonance imaging (MRI), more specifically, cardiovascular magnetic resonance (CMR) has seen significant advances in the last three decades, which paved the way for interventional applications using MRI [90–93]. MRI is a non-invasive and an ionisation free medical imaging technique that employs powerful magnets to produce a strong magnetic field (commonly denoted by B_0). B_0 aligns and precesses the hydrogen nuclei, which are abundant in the human body and have intrinsic magnetic properties, along its direction. When an additional radiofrequency (RF) field is applied perpendicularly to B_0, the precessing hydrogen nuclei are tipped out of their alignment with B_0. Once the RF pulse is switched off, the nuclei realign with B_0 and concurrently emit an electromagnetic signal, which is detected by the MRI's receiving coil. The detected signals are then processed to form an image of the scanned area. The time it takes for the nuclei to realign with the magnetic field, and the amount of signal emitted is dependent on the environment and the chemical composition of the molecules. Figures 7 and 8 illustrate the basic physics of MRI and its relevant terminology [94–97].

In addition to its non-invasive and ionisation-free nature, the previously described MR physics results in enhanced soft tissue visualisation [14, 98]. Furthermore, MRI can also provide functional information such as blood flow, tissue oxygenation, diffusion, perfusion, and mechanical properties of tissues (elastography). Magnetic resonance angiography (MRA) and MR-guided interventions (figure 9) in general are performed with gadolinium-based contrast mediums instead of the iodine-based contrast agents. Similar to fluoroscopy-based angiography, MRA also provides a precise assessment of blood vessels. Even though MRA avoids the usage of iodine-based contrast agents, gadolinium-based mediums should be applied with care as they may increase the risk of a rare but serious disease called nephrogenic sclerosing fibrosis (NSF) in patients with severe kidney impairment [99, 100]. However, it has been shown that MRI has the ability to

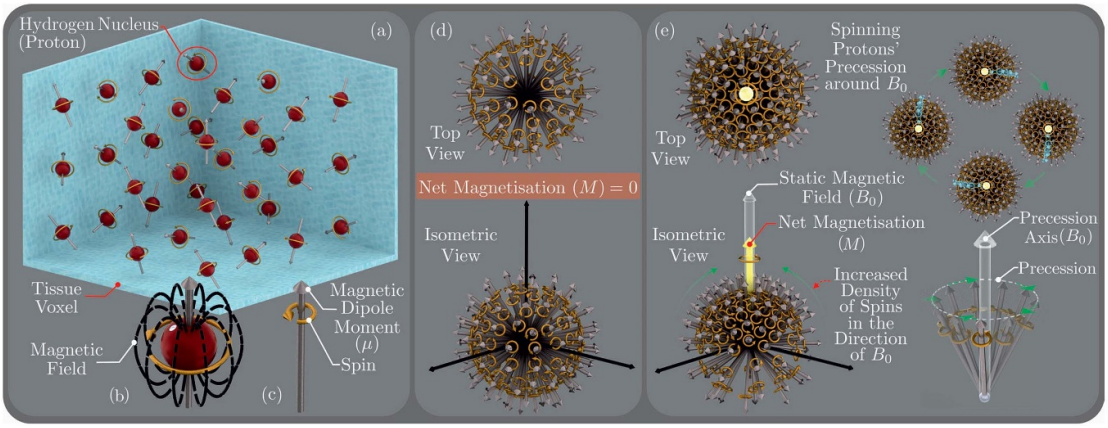

Figure 7. MR Physics (I): (a) A human tissue voxel largely made of water and fat, which contain hydrogen atoms. (b) A simplified representation of the nucleus of a hydrogen atom. The nucleus is a positively charged proton with an intrinsic property, called spin or intrinsic angular momentum. The non-zero net spin generates a magnetic dipole moment (μ or MDM for short), which in turn generates a small magnetic field. MDMs and spins are used interchangeably in literature because they track each other. (c) A further simplified representation of the nucleus, which is used in the rest of the figure. (d) In the absence of an external magnetic field, the atoms' MDMs are pointing randomly, hence giving a uniform distribution of MDMs in the top and isometric views of an implicit coordinate system. The net magnetisation (denoted by M) is the sum of the individual MDMs. In the absence of an external magnetic field, M is zero. (e) Upon the application of an external strong static magnetic field (B_0), i.e. the patient is placed in the MRI bore, two events take place: (1) The orientation of the MDMs is skewed slightly toward B_0's direction (increased density of MDMs) resulting in an increase in M (yellow arrow), (2) The ensemble of MDMs start precessing at the Larmor frequency (42 MHz at 1 Tesla) around B_0's direction. Although the spins are precessing, M remains in equilibrium.

perform angiography and endovascular interventions with only small amounts or even without the use of any contrast medium [100].

MRI provides anatomic and functional information on the target tissue but at a reduced spatial and temporal resolution when compared to x-ray fluoroscopy. Table 2 provides a brief overview of the spatial and temporal resolution of both X-fluoroscopy and MRA. For MR-guided endovascular interventions, the most widely used pulse sequence is the balanced gradient imaging technique, which is also known as TrueFISP (Siemens), FIESTA (GE), True SSFP (Toshiba), Balanced FFP (Philips) [105, 106]. This is primarily due to the sequence's relatively high signal-to-noise ratio (SNR) in short repetition time (TR) sequences [107]. TR is the amount of time between the application of an RF pulse and the start of the next RF pulse. Other equally fast MR sequences include: standard gradient-echo (GE or GRE) techniques which can be faster than the balanced gradient imaging technique and can be used to enhance and manipulate magnetic susceptibility artefacts, but tend to have an inferior SNR [107].

Despite its inherent potential, MR-guided interventions face a major challenge in the lack of MR safe and compatible instruments [14, 108]. Commercial catheters for navigation were designed for use under fluoroscopy guidance and cannot be used in an MR environment due to the frequent presence of long metal braids or coils along their shafts [9, 109]. Instead of directly guiding instruments under MRI, other research groups attempted combining x-ray fluoroscopy and MR-guided catheterisation (i.e. XMR procedures) by fusing a pre-operatively acquired MR image as an image overlay with real-time fluoroscopic images [110]. This provides a roadmap for guiding instruments in tortuous anatomies without the need for multiple contrast agent injections while lowering exposure time to ionising radiation. The drawback of this method, apart from still using ionising radiation, is the distortion of the anatomy caused by the interaction of stiff instruments with blood vessels; resulting in a significant incompatibility in the image overlay [14].

3.2. MRI safety labelling

As safety is a major concern in the development and application of medical devices for MR environments, it is important to understand the current classification of MR safety. To classify whether it is possible to use a device within an MR environment or not, the American Society for Testing and Materials (ASTM) devised a standard, namely ASTM F2503 [111]. This standard defines three possible classifications for medical devices used in MRI environments: MR safe, MR conditional and MR unsafe. The MR safe classification is assigned to devices composed of non-metallic, non-magnetic, and non-conductive materials by providing a scientifically based rationale rather than test data. Conversely, the MR conditional classification is assigned to an item with demonstrated safety in the MR environment within defined conditions (e.g. static magnetic field, the switched gradient magnetic field and the RF fields). The MR unsafe classification is designated to items which pose risks to the patient, medical personnel, or other persons within the MR environment.

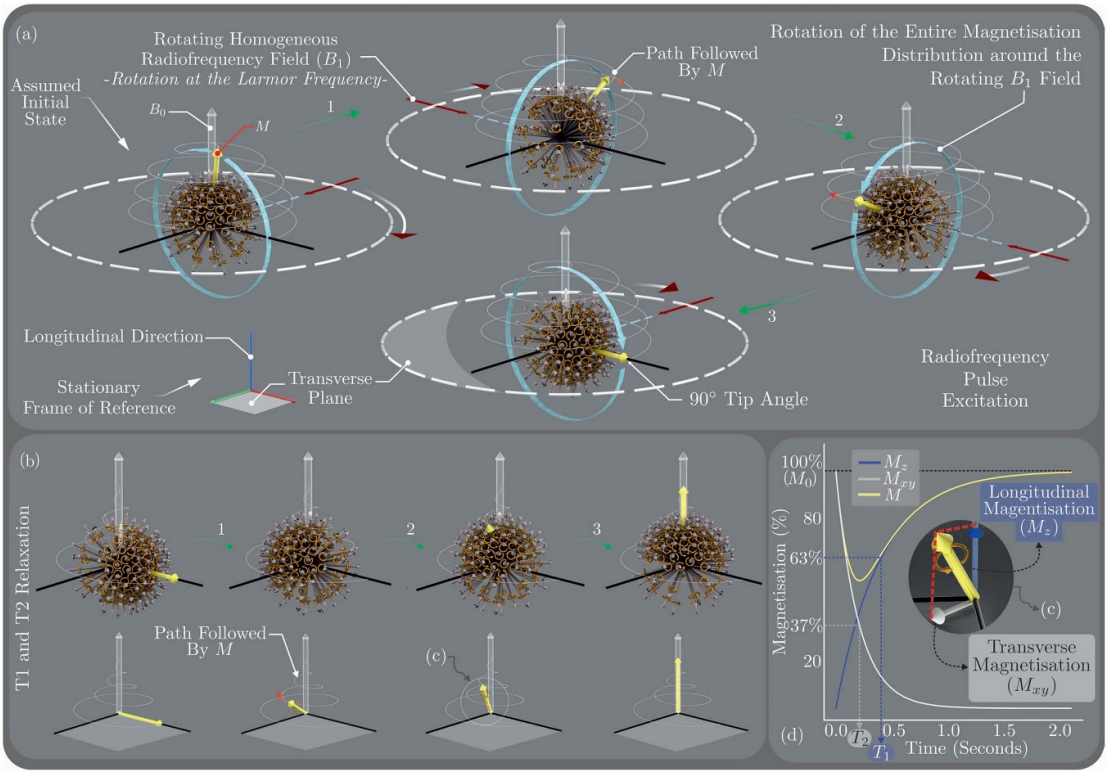

Figure 8. MR Physics (II): (a) RF Pulse Excitation: When a rotating homogeneous RF field, denoted by B_1 , is applied perpendicular to B_0, the entire magnetisation distribution, is tipped away from its initial alignment with B_0 (90° in this example). Simultaneously, the magnetisation distribution slowly rotates around the rotating B_1 axis (indicated by the blue circular arrow). Notes: the path followed by M is observed from a stationary frame of reference, B_1 field does not change the relative orientation of individual MDMs, and the B_1 field rotates at the Larmor frequency. (b) After switching off the rotating RF field, M returns to thermal equilibrium (relaxation), i.e. aligning back to B_0 direction. The inset (c) is zoomed-in in (d). (d) Plot illustrating the two magnetisation components of M, and their corresponding relaxation times. T_2 is the time required for the transverse magnetisation (M_{xy}) to decrease exponentially to approximately 37% ($1/e$) of its initial value. Conversely, T_1 is the time required for the longitudinal magnetisation (M_z) to return to 63% ($1 - 1/e$) of its maximum value (M_0), where M is equal to M_0 at equilibrium (i.e. aligned with B_0's direction). M_{xy} is the component detected by the RF receiving coils which gives rise to the MR image. M_z does not contribute to the acquired signals. An important mechanism for the decay in M_{xy} , i.e. T_2 relaxation (spin-spin relaxation) is as follows. The MDMs (spins) experience local fields which are combinations of B_0 and the fields from their neighbouring protons' MDMs. The variations in local fields lead to different local precessional frequencies, and as a result, the protons' MDMs (spins) fan out in time, thereby reducing M_{xy} . The fanning out of MDMs (spins) is referred to as dephasing. T_1 relaxation (spin-lattice relaxation), on the other hand, occurs when a proton exchanges magnetic energy with its external environment (lattice). T_1 relaxation also results in T_2 relaxation, ensuring that T_2 is longer than or equal to T_1. Note: The transition in (b) illustrates the overall effect of both relaxation mechanisms.

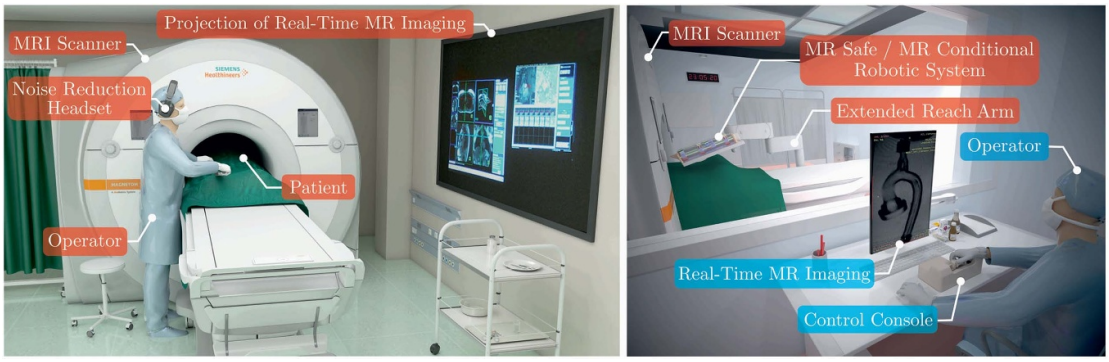

Figure 9. (Left) Hands-on MR-guided intervention: the operator manipulates the instruments manually with real-time MR images projected onto a screen inside the scanner room. Operators, staff, and patients wear noise reduction headsets to protect their hearing from the loud noises produced by the scanner's gradient coils [101]. (Right) Robotic-assisted MR-guided intervention: The operator uses a control console to remotely operate an MR safe/MR conditional robotic system which in turn manipulates the instruments. The operator can view the real-time MR images on the screen located in the scanner's control room [81].

Table 2. Temporal and spatial resolution of x-ray fluoroscopy vs MRA.

	Temporal resolution	Spatial resolution	Reference
X-ray fluoroscopy	30–260 ms	0.2–0.3 mm	[102]
MRA	52–292 ms	0.65–1.5 mm	[103]
	20–30 ms	1.5–2.0 mm	[104]

3.3. Guidewires and selective catheters

Guidewires: For the adoption of existing guidewires (figures 2–4) into MR environments, the long metal core wires commonly employed need re-evaluation. The non-ferromagnetic metal braids such as 304 V, 304 L, 316 L stainless steels, and nitinol [112, 113] create acceptable susceptibility artefact, i.e. MRI artefacts such as distortions and local signal change due to local magnetic field inhomogeneities. However, these are conductive metals which makes them intrinsically susceptible to RF-induced heating under MRI, risking thermal injury [109, 114]. The induced heating is a result of standing wave formation along the conductive parts longer than a quarter wavelength, which corresponds to approximately 12 cm in humans at 1.5 Tesla. To prevent RF induced heating, researchers explored using (extruded) PEEK-based passive [115] (figure 10(c)) and deflectable guidewires (figures 10(d) and (e)) [116]. In other instances, researchers repurposed a microcatheter by filling it is lumen with a low-viscosity resin microparticle compound to form a polymer-based guidewire [114]. Although simple in terms of construction, polymer only-based guidewires have lower bending stiffness when compared to their metallic counterparts [115]. This drawback led to the development of glass fibre-reinforced polymer-based guidewires which were found to have improved mechanical properties (i.e. improved kink resistance, flexural and torsional stiffness) [117–120]. In [100, 118, 121], Kos *et al* fabricated a glass fibre-reinforced PEEK core, a soft tip, polyurethane jacket and a hydrophilic coating. They utilised the (thermoplastic) micropultrusion process to fabricate the core material of the guidewire (figures 10(a) and (b)). To achieve the desired distal end flexibility (soft tip), they grounded the core to a desired profile. The guidewire was evaluated *in-vitro* and *in-vivo* under MR-guidance to demonstrate feasibility for stenting of iliac and supraaortic arteries [100], renal artery angioplasty [118], and percutaneous transluminal aortic stenting and cava filter placement [121]. In [119], Krueger *et al* fabricated a similar guidewire with a glass fibre-reinforced core wire. Instead of PEEK as the base material for the micropultrusion process, they used epoxy (thermoset micropultrusion). For distal end flexibility, the core wire was later attached to a nitinol soft tip (10 cm in length) and covered with a polyurethane jacket. This cover served as a base for coating the guidewire with a hydrophilic, biocompatible polymer [119]. The guidewire was evaluated in five pigs under MR-guidance by catheterising the carotid and renal arteries, segmental arteries of the kidneys, the contralateral inguinal artery, and the left ventricle. Several other interventional applications were also investigated such as balloon dilation, stent deployment and embolisation of small blood vessels [122]. To further evaluate its efficacy and safety, the guidewire was utilised to perform 20 cardiac interventions in five female domestic pigs, and two MR-guided balloon dilation of the pulmonary valves of two patients (a child and an adult) with congenital heart diseases (pulmonary valve stenosis). The preclinical and first-in-man trials results were encouraging, with no procedural complications for both patients [120]. It was subsequently realised whilst performing additional clinical trials that glass fibre-reinforced guidewires were prone to fracture during intervention as experienced by Pushparajah *et al* [123].

The risk of guidewire fracture led to the development of not only new fibre composites, utilising both glass and aramid fibres (Kevlar®), but also new manufacturing technologies based on micropultrusion, i.e. micro-pullwinding [129]. (Micro)pultrusion is a scalable process which allows for the production of fibre-reinforced composite material [119]. Depending on the base material to be reinforced, pultrusion can be further classified into the conventional thermoset pultrusion and thermoplastic pultrusion [130]. The process of thermoset pultrusion commonly starts by unwinding the fibres from spools, followed by pulling the fibres into a resin bath (e.g. epoxy) that saturates or wets out the reinforcement. The wet out reinforcements are then pulled into a heated pultrusion die to cure the finished part. Thermoplastic pultrusion on the other hand, involves the pulling the fibres into a pre-heated unit comprising the melt thermoplastic resin, followed by a die to consolidate the fibre/resin mass. The consolidated fibre/resin is then passed through a cooling device to ensure a dimensionally stable end product [130]. In attempt to manufacture guidewires with different mechanical properties along its length, the Fraunhofer IPT team developed the micro-pullwinding process [129], a process combining both pultrusion and filament winding. In this process, the pultruded profile (using glass fibres) is wrapped and consolidated with additional layers of high-strength synthetic fibres (e.g. Kevlar®) in several winding units to significantly enhance its torsional and radial stiffness (figures 11(f)–(i)) [129]. Moreover, since glass fibres are susceptible to buckling, the

Figure 10. MR Guidewires (I): (a) Guidewire consisting of a glass-fibre reinforced PEEK core covered with a polyurethane jacket. The core is grounded at its distal end to create a flexible distal end. (b) Cross-sectional (inset) of the micropultruded glass-fibre reinforce PEEK core [100, 118, 121]. (c) Guidewire comprising a PEEK core with iron microparticles embedded in the polymeric coating [115]. (d) Steerable guidewire composed of a flexible PEEK shaft, a deflectable tip and a Dyneema® tendon travelling through the entire guidewire. The steerable tip is a re-purposed 2.4Fr microcatheter (flexible tube) embedded with a flattened nitinol rod to straighten the tip and to constrain its bending in one direction. At the very distal end of the guidewire is a PEEK cap. The entire body is covered with polyethylene heat shrink tubing to hold all the components together. (e) Pulling of the tendon results in the bending of the deflectable tip [6, 116]. (f) Guidewire constructed using short nitinol rod segments (guidewire shaft) and a tapered nitinol rod with a long coil mounted onto it (flexible distal end). The distal end is jacketed with a non-braided thermoplastic polymer and the entire body is covered with a soft polymer. (g)–(h) Zoom-in cross-sectional (inset) of the guidewire shaft which consists of nitinol rod segments (grey) joined by nitinol connectors (blue) with notched ends. For electrical insulation, the nitinol rod is coated with a thin film of parylene and jacketed with PEBAX® to achieve a consistent profile (between rods and connectors) [124]. *MRI markers are passive (−ve).

wound layers provide protection in the case of accidental fracture. This process led to the development of a commercially available MR conditional guidewire EmeryGlide™ (Nano4imaging, Düsseldorf, Germany). The EmeryGlide™ comprises a high strength core composite of glass fibres and polymers, protected by a double winding of aramid fibres embedded in polymer. The full body is covered by a PTFE sleeve to minimise intravascular friction to protect the tip and shaft from breakage. To proof feasibility, Reddy *et al* used the guidewire in a pilot study performing real-time interventional cardiac magnetic resonance (iCMR) in a 1.5 Tesla system on 34 patients, with a success rate of 91% (31/34) [131]. In an attempt to mitigate the lack of MR compatible instrumentation, Nano4imaging recently signed a US distribution agreement with B. Braun Interventional Systems Inc. to sell their MR conditional guidewire to the US market.

Simultaneously, Wolska-Krawczyk *et al* used an MR conditional guidewire (EPflex, Dettingen an der Erms, Germany) to examine its heating and safety when compared to a standard nitinol guidewire (figure 11(e)). The MR conditional guidewire used consisted of (twisted) high-strength aramid synthetic fibres along its longitudinal axis, surrounded by a bending-resistant high performance polymer composite

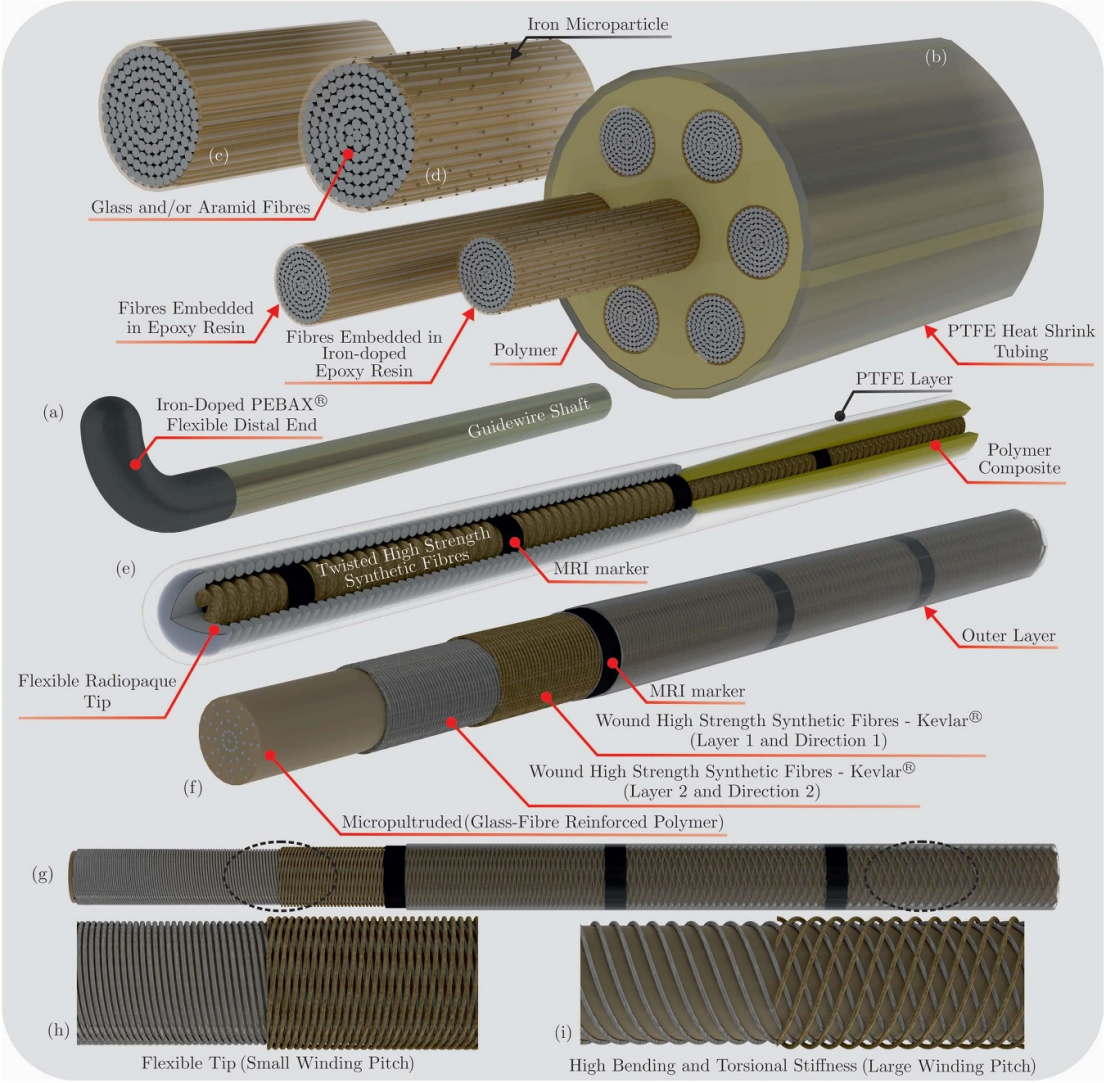

Figure 11. MR Guidewires (II): (a) Stiff MaRVis guidewire comprising of a shaft and an iron-doped PEBAX® flexible distal end. (b) Cross-sectional zoom-in (inset) of the shaft that consists of micropultruded glass or aramid fibres embedded in epoxy resin and in certain cases iron-doped epoxy resin for MR visibility (referred to as MaRVis rods). To construct the guidewire shaft, several MaRVis rods are arranged and embedded in a polymer matrix and are subsequently covered with a PTFE heat shrink tubing. (c) Further zoom-in (inset) of a MaRVis rod. (d) Further zoom-in (inset) of a iron-doped MaRVis rod [125, 126]. (e) Guidewire consisting of twisted high strength synthetic aramid fibres, surrounded by rings of passive negative markers for MR visibility (placed at discrete points) and a polymer composite to provide the desired mechanical performance. At the distal end, a flexible radiopaque tip is mounted at the tip for enhanced tip visibility. The entire body is covered with a PTFE heat shrink tubing. In [127, 128], instead of the coil and PTFE layer, the tip section was coated with PEBAX® and the guidewire was coated with a hydrophilic polymer. (f)–(g) Guidewire comprising a micropultruded glass-fibre reinforced core wrapped and consolidated with additional layers of high strength synthetic fibres. Passive negative markers are applied at discrete intervals for MR visibility and an outer layer is utilised to form the guidewire. (h) Flexible tip achieved by small winding pitch and (i) High bending and torsional stiffness of guidewire shaft achieved by large winding pitch [129].

and a PTFE layer. The tip section is conically tapered to create an atraumtic, and a radiopaque flexible tip [127, 128]. Their investigation showed insignificant temperature elevation during near-real-time MR sequences. A preclinical *in-vitro* (phantom) study was performed using the same guidewires to test the feasibility of a developed framework for guiding endovascular interventions in MR environments [132]. Further, a recent iteration of the EPflex MRLine guidewire was employed in the evaluation of an MR conditional cardiac phantom [133]. The phantom was developed as a training platform for interventional CMR procedures. The EPflex guidewire was also used in a comparative *in-vitro* study with x-ray fluoroscopy to evaluate its efficacy [134]. Five EPflex guidewires were used alongside one EmeryGlide™ guidewire in the right heart catheterisation of six patients (out of 50 patients in total) to investigate the association between catheterisation time and hemodynamic parameters in an MR setting [135].

The drawback of using polymeric materials is the poor visualisation and localisation in MRI environments due to their low magnetic susceptibility [14]. In order to visualise the previously described guidewires, passive negative markers are commonly employed. In the negative contrast approach, the

incorporated materials or added markers make guidewires visible by introducing localised magnetic field inhomogeneities which lead to the dephasing of adjacent proton spins and a local signal void (susceptibility artefact) on an MR image [136, 137]. The common method adopted by research groups and guidewire manufacturers involves the gluing or adhering (super)paramagnetic iron oxide microparticles embedded in curable resin at different (discrete) points along the length of the guidewire to provide better MR visibility. However, as indicated in [135], one of the limitations of using such discrete markers, is the inability to visualise the whole length of the guidewire as clinicians would normally do in a fluoroscopy setting. Moreover, this limitation is overcomed by the continuous visualisation of the MR Safe MaRVis guidewire (MaRVis Interventional GmbH, Krün, Germany), as a result of the centrally localised passive negative iron microparticles along the guidewire's length (figures 11(a)–(d)). The MaRVis guidewire comprises several thin rod-shaped composite material (MaRVis rods) embedded in a polymer matrix and covered by a PTFE sleeve. These micropultruded rods are composed of non-metallic filaments (e.g. glass or aramid fibres) impregnated by a high temperature resistant epoxy resin. For continuous MR visibility, some of the fibres are impregranted with epoxy doped with iron microparticles. The iron-doped rods tend to be placed at the centre of the guidewire to limit the size of the artefacts [125]. The MaRVis guidewires were thoroughly evaluated *in-vitro* (phantom models) and *in-vivo* [89, 126, 138]. The preliminary results reported by the three studies showed that the usage of the MaRVis guidewires in MR-guided interventions is technically feasible and safe in swine models and potentially, in humans.

Alongside these promising MR guidewires developments, Basar *et al* proposed using a segmented-core nitinol device construction, where they maintained less than one-quarter wavelength at 1.5 Tesla, which eliminates standing wave formation, and the possibility of RF heating along the shaft [124]. The guidewire's core consists of a 10 cm PEBAX®-coated nitinol rod segments joined by 5 mm connectors for stiffness matching. The shaft of the segmented-core assembly was covered by a liquid crystal polymer (Vectran™) fibre-braided polyimide tubing to enhance the guidewire's pushability, torque response, kink resistance, and dielectric properties. For the distal end, a tapered nitinol rod was employed, with a coaxially placed 3 cm support Nickel–Cobalt–Chromium–Molybdenum alloy coil ((MP35N alloy), Heraeus, MN, USA) to enhance the tip's flexion and recoil [124]. The distal end was covered by a non-braided thermoplastic polymer to ensure softness and flexibility. The guidewire was visualised under MR by placing passive negative iron oxide markers at 10 cm intervals. The entire guidewire assembly was then covered by a thermoplastic jacket to avoid blood contact and to achieve a standard outer diameter of 0.035" (figures 10(f)–(h)). To compare the MR segmented guidewire with a commercial nitinol guidewire, the MR guidewire was mechanically characterised and test *in-vitro* and *in-vivo* in an MR setting. The passive guidewire exhibited similar mechanical behavior to its commercial counterpart, with a significant drop in guidewire heating from 13° to 1.2° [124]. Table 3 provides an overview of the materials employed in the construction of the previously described MR safe and MR conditional guidewires, and their structural strengths and weaknesses.

Selective Catheters: To prevent RF induced heating in selective catheters, researchers explored substituting metal braids with non-metallic, non-conductive polymeric braids, such as aramid fibres (e.g. Kevlar®) in selective catheters [89]. As in the case of guidewires, replacing metallic braids (figure 6(c)) may also result in the reduction of the overall mechanical performance (flexibility, torquability, pushability) of catheters [139], and limit their appropriateness for interventions. Similar to the previously described nitinol rod segmentation approach [124], Yildirim *et al* proposed a promising alternative technique to modify braided selective catheters by creating discontinuities within the insulated metal wires to limit RF induced heating while preserving their mechanical properties and kink resistance [109].

3.4. Steerable catheters

In parallel to the advancements in MR guidewires and MR selective catheters, a plethora of work has been conducted in the field of 'MR safe' and 'MR conditional' steerable catheters for MR-guided interventions. The following summary of findings is classified based on the actuation mechanism. The summary will cover the steerable catheters developed both for guiding intravascular devices and for the treatment of atrial fibrillation (electrophysiology). In addition, table 4 provides an overview of the materials employed in the construction of the following steerable catheters.

3.4.1. Tendon(s)

Tendon-driven steerable catheters are generally constructed from a stiff shaft and a compliant distal end. To steer the distal end, high strength, polymeric tendons are incorporated in the catheters, travelling from the proximal end through the stiff shaft to the flexible distal end. The push/pull movement of the tendons causes the tip to deflect. The simplest form of tendon-driven catheters is demonstrated by Bell *et al*, where they developed a uni-directional tendon-driven steerable guiding catheter. Their catheter is composed of a proximal shaft with Kevlar® braiding encapsulated between an inner PTFE liner and an outer thermoplastic

Table 3. Materials used for constructing guidewires for MR-guided interventions. Markers: passive negative marker (PN), passive positive marker (PP), semi-active tracking (SA), indirect active tracking (IA), direct active tracking (DA).

	Ref	Materials used (function)	Marker	Pros and cons
MR Guidewires	[115]	Distally tapered PEEK rod (core), synthetic material embedded with iron microparticles (coating)	PN	+ Simple construction − Lower bending stiffness
	[116]	(Proximal Shaft): PEEK Tube (core), Polyehtylene (PE) heat-shrink (outer layer), (Distal End): Repurposed 2.4 Fr microcatheter (steerable tip), Flattened nitinol rod (Straighten the tip & Constrain bending to one plane), (Entire Guidewire): Dyneema® (pull-wire)†	PN	
	[117]	Glass fibre-reinforced guidewire	PN	+ Improved mechanical
	[100, 118, 121]	Distally tapered, micropultruded glass fibre-reinforced PEEK rod (core), Polyurethane (jacket), Hydrophilic polymer (coating)	PN	properties (i.e. improved kink resistance, flexural and torsional stiffness) − Risk of fracture
	[119, 120]	(Proximal Shaft): Micropultruded glass fibre-reinforced epoxy rod (core), (Distal End): Cone shaped nitinol wire (flexible distal end), (Entire Guidewire): Polyurethane (jacket)†, Hydrophilic biocompatible polymer (coating)	PN	
	[129]	Micropultruded glass fibre-reinforced polymer (core), Wrapped and consolidated Kevlar fibres® using the filament winding process (protection from accidental fracture and enhancing torsional/radial stiffness) → Nano4imaging employs a similar construction in their EmeryGlide™ guidewire	PN	+ Different mechanical properties along the length + Significantly enhanced torsional and radial stiffness + Decreased Risk of fracture
	[127, 128]	Twisted high-strength aramid synthetic fibres (core), Distally tapered bending-resistant high performance polymer composite (core support), PTFE heat-shrink tubing (outer layer), Radiopaque flexible tip (tip visibility) → EPflex employs a similar construction in their MRLine guidewire	PN	
	[125, 126, 138]	Micropultruded rod-shaped composite material (aramid/glass fibre), polymer matrix, PTFE heat-shrink sleeve (outer layer), (Distal End): PEBAX® embedded with iron microparticles → MaRVis Interventional GMBH employs this construction in their MaRVis guidewires	PN	+ Continuous visualization along the whole length

(Continued.)

Table 3. (Continued.)

Ref	Materials used (function)	Marker	Pros and cons
[124]	(Proximal Shaft): 10 cm PEBAX®-coated nitinol rod segments joined by 5 mm nitinol rod segments for stiffness matching (core), Liquid crystal polymer (Vectran™) braided polyimide tubing (jacket), (Distal End): Tapered nitinol rod (flexible tip), Nickel-Cobalt-Chromium-Molybdenum Alloy coil (enhance tip's flexion and reocil), Non-braided thermoplastic polymer (jacket)	PN	+ Enhanced pushability, torque response, kink resistance, and dielectric properties
[140]	(Proximal Shaft): Laser cut nitinol hypotube (outer tube), (Distal End): Copper solenoid coil (tip tracking) (Entire Guidewire): Nitinol rod (core and loopless antenna), Polyimide tube (accommodate temperature probe), PEBAX® tube (first insulation cover), PEBAX® tube (Outer insulation layer)	IA	+ Comparable flexibility to commercial nitinol guidewires

polyurethane (Pellethane®) layer. For the distal end, they used a 5 cm nitinol laser-cut hypotube supported by a nitinol spring to provide kink resistance and to help restore the distal end shape upon release of the 0.38 mm Kevlar® tendon (figure 12(a)). To form a unitary catheter, the entire assembly was covered by PEBAX® tubing. The catheter was controlled using a custom-made 3D printed manual handle, which incorporated a distal end shape locking mechanism. In addition to mechanically assessing their catheter, they investigated three MR visualisation strategies (*in-vitro* and *in-vivo*); with active tracking providing the best visibility [141]. Yao *et al* followed a similar catheter construction to [141], where they utilised a nylon braided shaft glued to a nitinol-supported PTFE deflectable distal end. To steer the distal end, a 0.5 mm carbon fibre rod travelling from the manual handle through the shaft is glued to a thinner (0.25 mm) carbon fibre wire travelling from the shaft's distal end to the tip of the deflectable section (figure 12(b)). They benchmarked their catheter's mechanical performance alongside three commercial MR unsafe ablation catheters by performing *in-vitro* flexibility, torquability and pushability tests. Furthermore, they attempted a preliminary MR compatibility test by placing the catheter in a contrast-enhanced medium [142].

A drawback of steerable catheters with single deflectable segments is their inability of mimicking the shapes of commonly used pre-curved selective catheters, such as Headhunter1 (H1), Sos Omni, Simmons2 (SIM2), Judkins Right 4 (JR4) and Renal Double Curve (RDC). Such selective catheters have primary, secondary and in some instances tertiary curves formed onto their distal ends to facilitate navigation through the aortic arch and subsequent blood vessels. Figure 6(i) illustrates the two curves of a Judkins right catheter. To tackle this challenge, Clogenson *et al* proposed a steerable catheter with two independent deflectable sections which can be manually controlled using four ultra-high molecular weight polyethylene Dyneema® tendons [6, 7]. The catheter was constructed using a monolithic approach, where a subtractive manufacturing method was employed to laser profile the distal end of an inherently stiff extruded polymeric tube (polyether ether ketone (PEEK)). Thereby, creating an articulated structure where the links or hinges of the structure are interlocked and move with respect to each other when the tendon is pulled (figure 12(c)). In order to better visualise the catheter under MRI, paramagnetic iron oxide microparticles (1–6 μm) were glued at three different points along the distal end of the catheter. The handle/catheter assembly was evaluated *in-vitro* in a 1.5 Tesla MRI scanner, and *in-vivo* in a 3 Tesla MRI scanner. As reported in [6, 7], the main limitation of their design is the difficulty in controlling the two segments independently, i.e. steer one segment without involuntarily moving the other. This is caused by the change in length of a segment's tendon when the other segment is being steered. One way to avoid such undesired motion would be to compensate for this change with the manual control handle.

In line with robotic endovascular interventions, an alternative design was proposed where two catheters, each with its own single deflectable segment are placed over one another, referred to as 'concentric or telescoping catheters'. This method not only improves controllability, it also increases the number of degrees

Table 4. Materials used for constructing steerable catheters for MR-guided interventions, *patents are excluded, † Extends to the distal end, ‡ Only discussed in reference, marker: passive negative marker (PN), passive positive marker (PP), semi-active tracking (SA), indirect active tracking (IA), direct active tracking (DA).

		Ref	Proximal end material (function)	Distal end (function)	Marker‡
Steerable Catheters	Tendon(s)	[141]	PTFE (inner liner), Kevlar® (braiding), Pellethane® (outer layer), PEBAX® jacket (outer cover)†, Kevlar®	Laser-cut nitinol slotted tube (steerable tip), Nitinol Spring (kink resistance, shape restoration), Polyolefin heat-shrink tubing (outer layer),	PN, SA, IA
		[142]	Nylon braided tubing, Carbon fibre (pull-rod, pull-wire)†	PTFE multi-lumen tubing (steerable tip), Nitinol ribbon (kink resistance)	—
		[6, 7]	PEEK multi-lumen tubing (base), Nitinol rod (additional stiffness), Polyethylene (PE) heat-shrink tubing (outer layer), Dyneema® (pull-wire)†	Laser-cut distal end of PEEK multi-lumen tubing (steerable tip), Relatively thicker and more flexible polyolefin heat-shrink (outer layer)	PN
		[144, 145]	Monofilament braided tubing (catheter shaft), Polyethylene Fibre (steerable tip pull-wire)†, Glass fiber (carbon-fibre control wire)†	3D Printed Acrylonitrile Butadiene Styrene (ABS) segments (steerable tip), Flexible guide tube (inner layer), Sliding carbon fiber tube (inner tube, deflectable segment control), Central carbon fiber rod (stiffness enhancement)	—
	Hydraulic	[146]	Teflon tubing	Laser-cut nitinol tube (steerable tip), Silicone rubber tube (cover)	—
		[147–149]	Polymeric tubing†, Saline (drive fluid)†	Moulded silicone bellow (steerable tip), Hybrid micro stereolithography of UV curable epoxy resin (valve)	—
		[153]	—	3D Printed Polyethylene terephthalate glycol (PETG) (steerable tip), Silicone tubing (cover)	—
	Magnetic	[155]	—	Copper wire (coil)	DA
		[156]	2.7 Fr microcatheter†	Copper microcoils laser lithographed onto a polyimide tube and an alumina tube (coil), Heat-shrink tubing (outer layer)	—
		[158, 159]	2.9 Fr microcatheter (PEEK braided)†	Microcoils laser lithographed onto an alumina tube (coil), Heat-shrink tubing (outer layer)	DA

(Continued.)

Table 4. (Continued.)

	Ref	Proximal end material (function)	Distal end (function)	Marker‡
	[160, 161]	—	Silicone tubing (steerable tip), Copper wire (coil)	—
	[162]	Experiment 1: 5 Fr Catheter†, Experiment 2: Balloon Catheter†	Experiment 1: Cubic neodymium (NeFeB) magnets , Experiment 2: Fe_3O_4 ferrofluid (balloon catheter fluid)	NP
	[163, 164]	2.5 Fr microcatheter & Guidewire†	Ferromagnetic chrome steel bead (magnet)	NP
	[165]	8 Fr catheter†	Silicone tubing (steerable tip), Ferromagnetic high carbon bearing steel (SUJ2 − magnet)	NP
Shape Memory Alloy	[178]	—	Glass-silicone stacked three-dimensional structure (links), Nickel thin film deposited on a Parylene coated SMA coil (actuator)	—
	[179]	—	SMA coils (actuator), Silicone tubing (cover)	—
	[180]	—	Biomedical engineering plastic and brass (links), Parylene and polyurethane coated SMA Spring (inner tube), Parylene thin film (outer layer), Silicone rubber tube	—
	[181]	—	Electrochemically etched nitinol SMA sheet (actuator) and Nitinol tube (bias spring), Silicone rubber tube (cover).	—
	[182]	Polyethylene double lumen tube (inner tube)†	Electrochemically etched nitinol SMA sheet (actuator), Polyurethane tube (outer cover)	—
	[183]	—	SMA wires (actuator)	—
	[184]	PTFE tubing (inner)†, PTFE multi-lumen tubing (outer)†	SMA wires (actuator)	—
	[185, 187]	—	Nitinol wire (central beam), SMA wires (actuator), 3D Printed Acrylic plastic (collets)	—
	[192]	3D printed plastic tube	SMA wires (actuator), Nichrome wires (SMA wire heating)	—
	[163]	—	Radifocus® Guidewires (core structure), SMA wires (actuator), Isolated copper wires (SMA wires fixation)	—

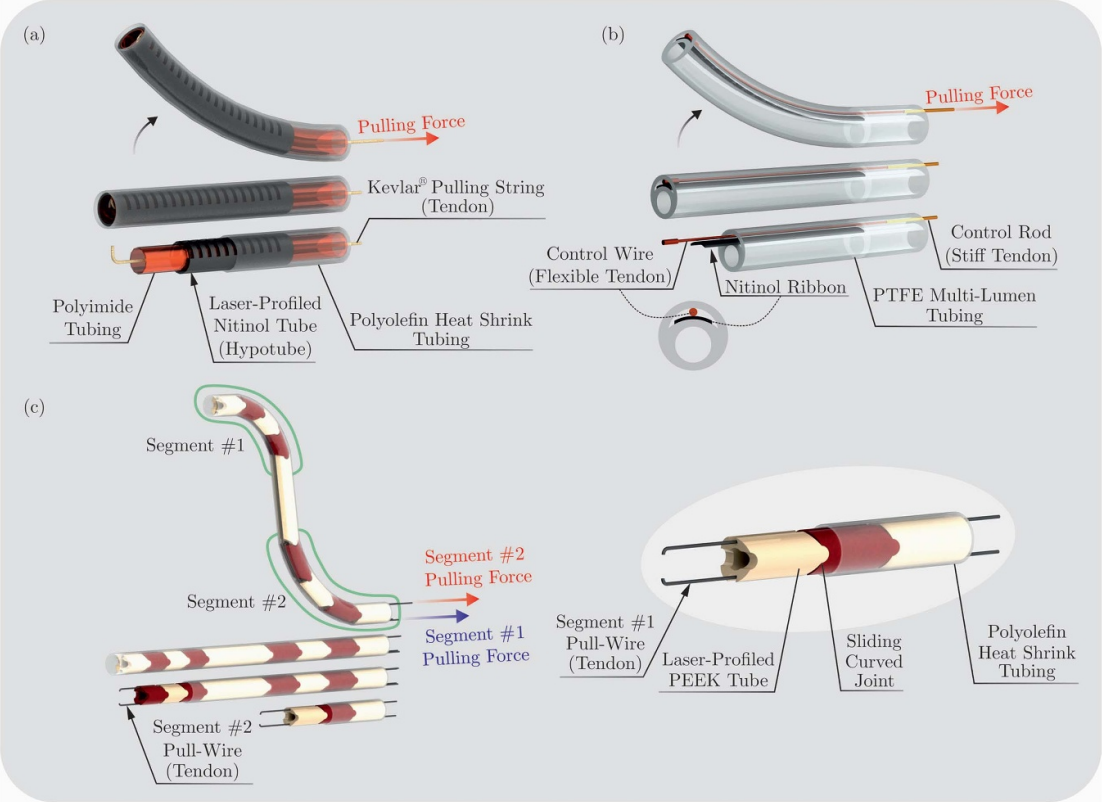

Figure 12. (Manual) Tendon Driven Catheters for MR-guided interventions (I). (a) A uni-directional catheter inspired by Bell *et al*'s design: The deflectable distal end consists of a nitinol laser-cut hypotube, connected to a Kevlar® tendon. In the case of Bell *et al*, a nitinol spring was concentrically added to the laser profiled tube [141]. (b) Yao *et al*'s uni-directional steerable catheter: A nitinol supported PTFE tube was used as the deflectable distal end. A control wire glued to a control rod was used for steering [142]. (c) Clogenson *et al*'s multi-selective catheter: The design comprises a laser profiled PEEK tube with four tendons travelling through the entire catheter length. The first pair of tendons control segment#1 and the second pair of tendons control segment#2. In terms of joint design, a sliding curved joint was utilised to form the articulated deflectable segments [6, 7]. Note: The catheter is made from a single material, however, different segment colours (red and beige) are used only used for illustrative purposes.

of freedom (DOF) [143]. Due to the unavailability of an MR compatible embodiment, the only example of this type is the fluoroscopy-guided Magellan 9Fr and 10Fr robotic catheter systems (AurisHealth, Redwood city, CA, USA). The 9Fr version released 2012, consisted of an inner leader catheter and an outer guide catheter. The leader catheter consists of four tendons articulating the single distal segment in two directions (bi-directional) and accommodates a standard 0.035" guidewire. Similarly, the guide catheter is bi-directional and fits around the leader catheter. With this configuration, both catheters are independently and collaboratively controlled to recreate the shapes of common selective catheters (figure 13(a)).

For MR-guided robotic endovascular interventions, Ataollahi *et al* explored the benefits of additive manufacturing by 3D printing steerable catheter distal ends (figure 13(b)). Their design comprised clockwise and counterclockwise helical segments employed in an alternating fashion [144, 145]. A distinctive feature of helical structures is the possibility of adjusting the stiffness of the deflectable distal end by tensioning all tendons simultaneously. To evaluate the deflectable segment's workspace and positioning accuracy in 3D space, the prototype was connected via four UHMWPE Spectra® tendons to an 'MR unsafe' robotic system. Further, *in-vitro* tests were performed to evaluate the segment's MR-compatibility and visibility.

3.4.2. Hydraulic

Hydraulically driven catheters (HDCs) are controlled by single or multiple pressurised tubes that run to chamber(s) of a soft and flexible distal end. Once a chamber is pressurised with fluid (e.g. saline), the catheter's distal end bends accordingly. Although not clearly stated by some of the authors who developed HDCs [146, 147], these catheters are good candidates for MR-guided interventions, due to the absence of 'MR unsafe' components in most of their constructions. Haga *et al* developed a 0.94 mm diameter uni-directional HDC by using a laser profiled nitinol tube covered with a thin silicone rubber tube and connected to a 2 m long PTFE tube [146] (figure 14(a)). They controlled the bending angle of the distal end by changing the negative pressure of the water in the catheter. Ikuta *et al* developed a 'single-input, multi-output' control mechanism to bend a multi-segment distal end [147–149] (figure 14(e)). Their

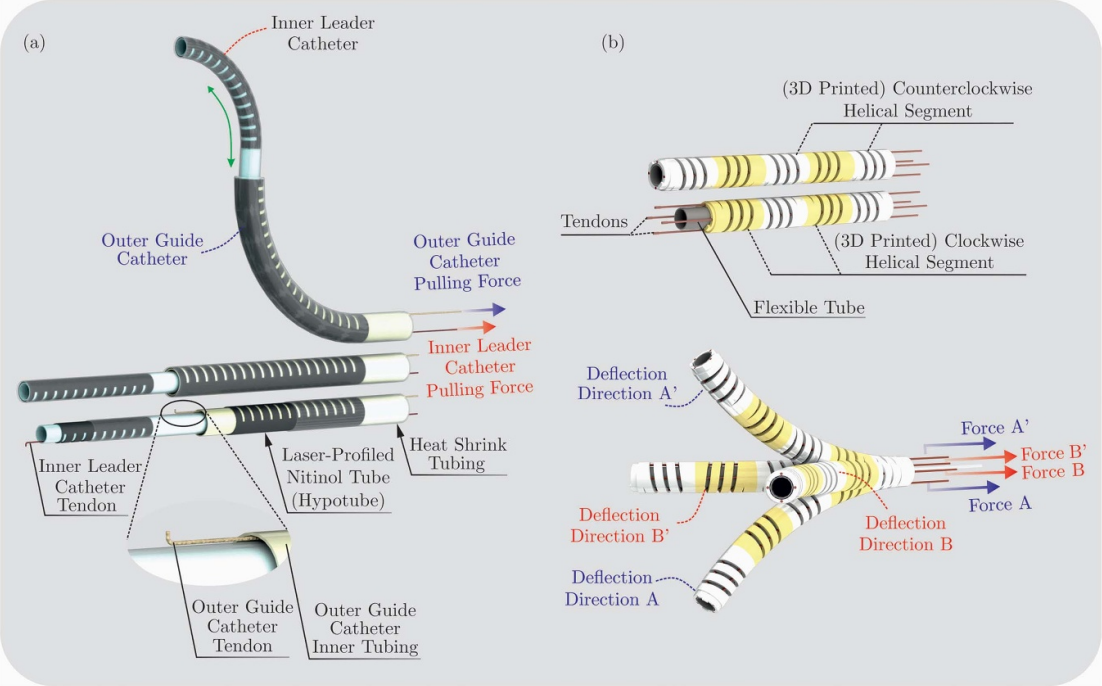

Figure 13. (Robotic) Tendon Driven Catheters for MR-guided interventions (II). (a) Simplest form of concentric or telescopic catheters: the system consists of two uni-directional catheters (inner leader catheter and outer guide catheter) which are controlled independently and collaboratively to recreate the shapes of common selective catheters. (b) Ataollahi *et al*'s additively manufactured deflectable catheter: The design consists of clockwise and counter-clockwise helical segments employed in an alternating fashion (illustrated in yellow and white). To control the distal end in 3D space, four polymeric tendons were utilised [144, 145].

catheter's distal end consisted of serially placed, independently valve-controlled bellows. Stereolithographed band pass valves (BPVs) were fabricated to control the fluid flow between the single pressurised-tube and the bellow it is attached to. Each BPV's inner pressure range is set at a unique value to enable independent control of each segment. To bend a specific segment, the target valve is opened by increasing the pressure of the tube until it reaches the activation pressure band of the walls of the deflectable segment, each filled with a pressurisable fluid (figure 14(b)). Changing the inner fluid pressure creates bending in a specific direction [150]. Actuation using inflatable balloons attached to the internal [151] (figure 14(d)) and external [152] (figure 14(c)) surfaces of the catheter's deflectable segment have also been proposed. Caenazzo *et al* proposed multi-functionalising the fluid used within the chamber of a 3D printed deflectable segment (inspired by Haga *et al*'s design) [153]. In their preliminary study, they employed conductive fluids (hypertonic saline solution) to replace the low-impedance wires used in steerable diagnostic and ablation catheters (figure 1(b)). This stemmed from the fact that wires tend to heat and cause significant artefacts in MR-environments.

3.4.3. Magnetic

Magnetic actuation is based on the changes in the magnetic field applied to the distal end of catheters having magnetic or electromagnetic elements. However, the previously mentioned remote magnetic navigation systems are inherently incompatible for use in MR-environments [154]. Roberts *et al* explored the use of the MRI scanner per se, to steer the distal end of catheters with copper coils wound around its tip [155] (figure 15(a)). In their design, the coils at the catheter's distal end generate a magnetic field when electric current is passed through it. As a result, when placed in the MRI's strong magnetic field (1.5 Tesla or 3 Tesla), the coiled distal end experiences a turning force or torque to align its magnetic field with the external field of the MRI scanner [155]. To achieve remote control in 3D space and reduce resistive heating, the authors improved their design by fabricating solenoidal microcoils by laser lathe lithography on polyimide and alumina substrates [156, 157]. In [156], *in-vitro* and preliminary *in-vivo* tests were performed to evaluate the resistive heating of the microcoils. To further assess their catheter's feasibility under real-time MR-guidance, *in-vitro* [158] and *in-vivo* (renal artery embolisation) [159] studies were performed. In both studies, the tests were compared with standard x-ray fluoroscopy guidance to determine the value of MR-guidance. The results of both studies show that MR-guided navigation is comparable to its fluoroscopy-guided counterpart. Liu *et al* proposed a design optimisation process for MRI-actuated catheters based on task and anatomical constraints [160]. In efforts to (semi-)automate catheter ablation procedures, Greigarn *et al* developed a

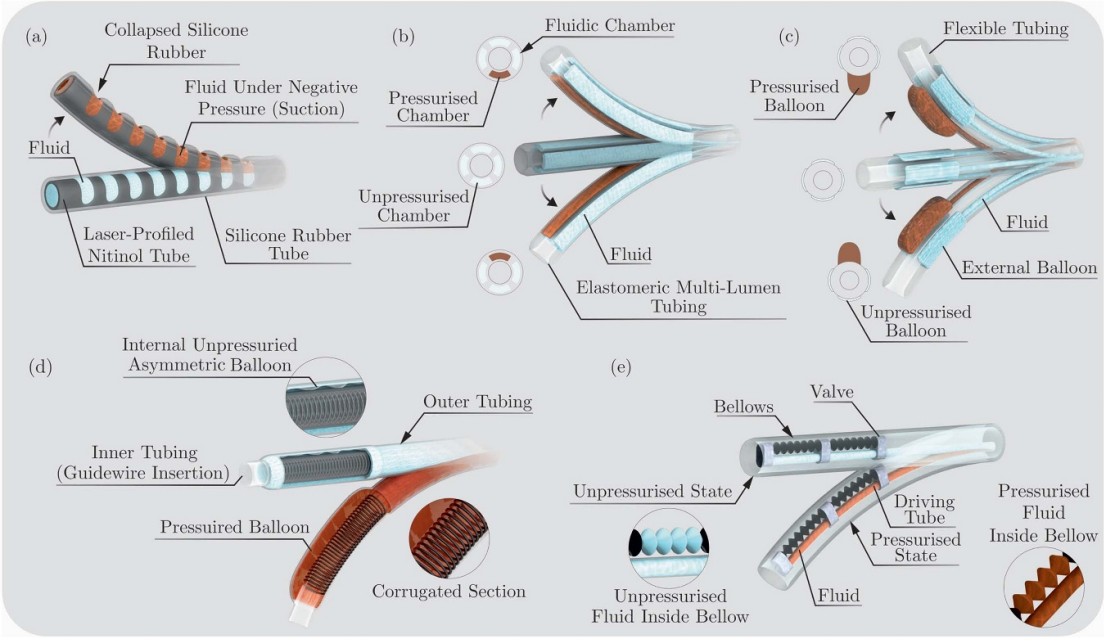

Figure 14. Distal end of Hydraulic Driven Catheters (HDCs). (a) Haga *et al*'s uni-directional HDC: A laser profiled nitinol tube covered with a thin silicone rubber tube is controlled by changing the negative pressure of the fluid [146]. (b) De Boer *et al*'s conceptual design of a multi-directional HDC: the distal end comprises a central lumen and four parallel pressurisable chambers. Changing the inner fluid pressure results in the bending of the deflectable tip of the catheter. Note: The figure illustrates deflection in only two directions [150]. (c) Skerven *et al*'s conceptual design of a multi-directional (External Balloon) HDC: the deflectable tip consists of four external balloons attached to a flexible tubing. To steer the distal end towards a specific direction, the external balloons are inflated (pressurised) and deflated (unpressurised) accordingly. Similar to De Boer *et al*'s design, the figure illustrates deflection in only two directions [152]. (d) Johansen *et al*'s conceptual design of an (Internal Balloon) HDC: The distal end includes a corrugated section attached to the inner tube and an asymmetric internal balloon attached to the outer tube. The internal balloon is configured to deflect the distal end of the catheter [151]. (e) Ikuta *et al*'s single-input, multi-output HDC: The steerable tip consists of serially placed, independently valve-controlled bellows. To bend a specific segment, the target valve is opened by increasing the pressure of the driving tube until it reaches the activation pressure band of the valve. The figure illustrates the case where both segments (bellows) are actuated [147–149].

mathematical model for MR-actuated catheters and designed a motion planning algorithm to generate desired catheter distal end trajectories [161]. Concurrently, several other groups demonstrated feasibility by using a catheter tip equipped with ferromagnetic spheres (figure 15(b), e.g. neodymium NeFeB [162], chrome steel [163, 164], bearing steel SUJ2 [165]) and, in other instances, ferrofluids [162] (figure 15(c)) instead of the aforementioned microcoils. One of the main challenges behind magnetic actuation is the size of the artefact caused by the presence of a ferromagnetic body within the MRI bore. Moreover, this artefact makes it difficult to visualise the surrounding soft tissue structures [164].

A unique feature of magnetic actuation, which differentiates it from other actuation mechanisms investigated in this review, is that it does not need a physical connection. Thanks to this feature, in addition to tethered applications (i.e. MR-actuated catheters), magnetic actuation also allows remote powering facilitating navigation of untethered objects. While actuation mechanisms of tethered systems can utilise large Lorentz forces, the untethered particles in the absence of current need to rely on gradient pulling forces. This untethered powering of ferrous (ferromagnetic) particles, as stated in the review paper [166], is a great advantage as it allows miniaturisation of the ferromagnetic particles, enhancing the navigation potential under MRI to reach challenging targets or increase the efficacy of the procedures. Millimetre size robots encapsulating ferrous beads are proposed to introduce orientation-dependent tasks [167, 168] and therapeutics [169, 170]. This gradient pulling actuation method for untethered particles usually targets interventions involving embolisation procedures with the help of the materials loaded to these particles [171–173]. More sophisticated structures involving magnet to magnet interactions for particles that could still be navigated under MRI have been investigated for purposes like drug delivery [174, 175] and tissue penetration [176].

3.4.4. Shape memory alloys (SMAs)

Shape memory alloys are a unique class of material which exhibit the shape memory effect, an effect which occurs when a material deformed at low temperature reverts to its prior shape upon heating above a temperature characteristic of the alloy at hand [177]. The most prevalent SMAs are the nickel-titanium

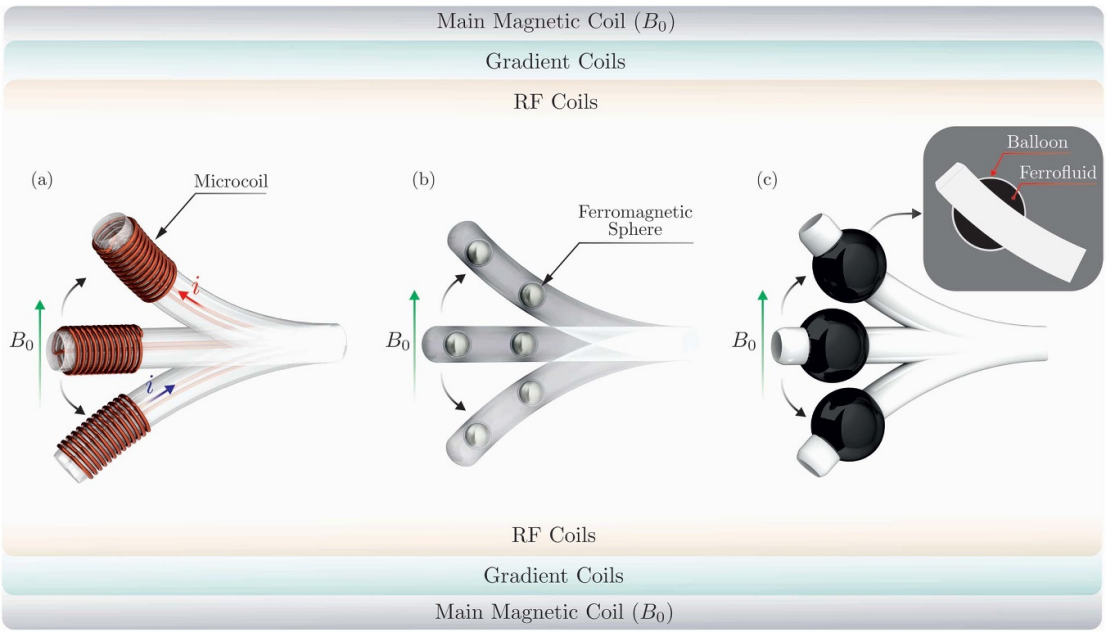

Figure 15. Distal end of MR-actuated Magnetic Catheters (a) (Simplified, Single Plane) microcoil-based: a microcoil is attached to a flexible tubing. Depending on the direction of flow of current, the distal bend is steered in a specific direction accordingly [155–161]. (b) Ferromagnetic sphere-based: The deflectable tip consists of ferromagnetic spheres [162–165]. (c) Ferrofluid-based: The distal end comprises a balloon filled with a ferrofluid [162]. All three distal ends (a)–(c) experience a turning force or torque to align its local magnetic field with the external field of the MRI scanner. The distal ends in the figure are placed within the bore of the MRI scanner, indicated by the three main components: main magnetic coil, gradient coils and RF Coils.

(nitinol) alloys, which are commonly employed as actuating elements in steerable catheters. SMA actuators can be in the form of microcoils [178–180] (figure 16(a)), electrochemically etched sheets [181, 182] (figure 16(b)), wires [183–187] (figure 16(c)), and laser cut tubes [188–191] (figure 16(d)). To bend the catheter's distal end, SMA actuators are often placed at an offset from the catheter's central axis in their deformed martensite phase. When the SMA actuators are heated, either by joule, optical or conductive heating, the actuators return (contract) to their high temperature austenite phase. Upon passive cooling, the SMA actuators extend back to their deformed martensite phase. As in the case of hydraulic actuation, most of the previously proposed works do not discuss the potential of MR-guided interventions, although nitinol based SMAs have an acceptable susceptibility artefact. Recently, Sheng *et al* developed an SMA actuated steerable catheter to treat atrial fibrillation under MR-guidance [192]. In their design, the distal end of their catheter consisted of multiple bending modules, with each module being actuated by a pair of antagonistic SMA wires. To actuate the SMA wires, conductive heating was implemented by routing nickel-chromium (nichrome) coils around the SMA wires. The steerable catheter was evaluated by performing *in-vitro* phantom tests and preliminary MR-compatibility experiments.

3.4.5. Comparison

Each actuation method has its own set of strengths and limitations. To comparatively assess the aforementioned steering mechanisms, the following categories are considered: steerability and safety. Table 5 summarises the comparison.

3.4.5.1. Steerability

Tendon-driven catheters are generally lightweight, manually controllable and can be swiftly manoeuvred when compared to other methods. Their main challenge lies in the mechanical nonlinearities experienced with an increase in the number of moving components and DOF [15]. Examples of such nonlinearities include friction between tendons and their corresponding catheter lumens; and the backlash caused by tendon slack and moving components of the tendon driving mechanism (e.g. gears). Other challenges include the uncontrolled change in length of tendons caused by the passive bending of catheter shafts while manoeuvring through tortuous anatomies. In the case of HDCs, the use of incompressible fluids facilitates the smooth motion and precise control of deflectable segments [193]. Nevertheless, fluidic actuation presents several drawbacks such as slower response times when compared to tendon-driven catheters; the need for equipment like pumps, valves and pipes; the possibility of leakage which can limit the catheter's efficiency [194]; the need for sophisticated control methods [193, 195]; and difficulty in miniaturisation

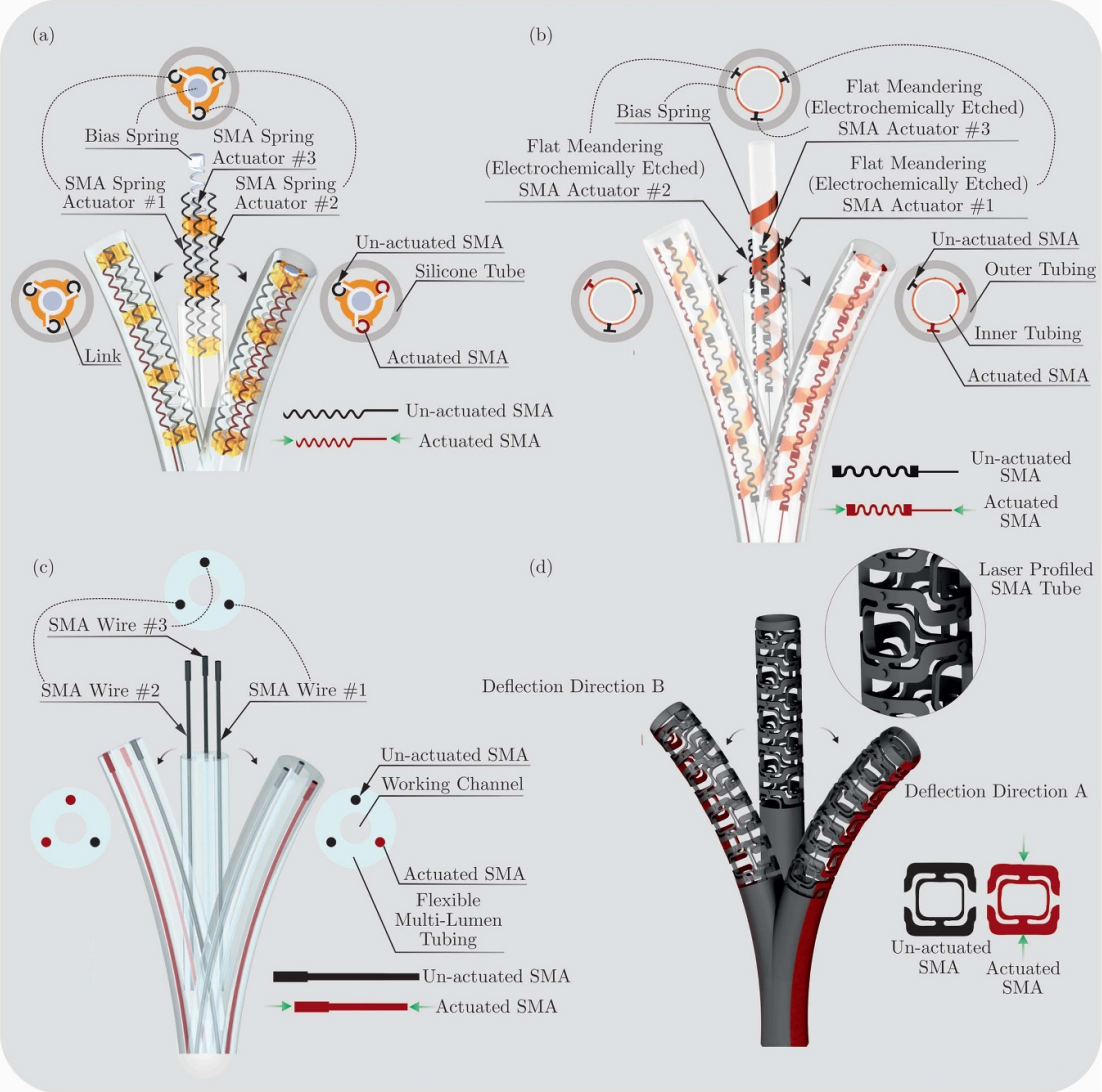

Figure 16. Distal end of shape memory alloys (SMAs) actuated catheters. (a) SMA Microcoils/Springs (Fu *et al*'s design): this design comprises three microcoil actuators, a bias spring and links (to fix and integrate the SMA actuators and bias spring). A silicone tube was utilised to cover the entire configuration [178–180]. (b) Electrochemically etched SMA sheets (Mineta *et al*'s design): an SMA sheet was electrochemically etched into SMA (flat-spring-like) actuators, which were then attached to a helical bias spring. To form a unitary body, an outer tubing was employed, and inner tubing was added to facilitate the insertion/removal of guidewires and intravascular devices. Namazu *et al* utilises similar fabrication and actuation techniques [181, 182]. (c) SMA wires: In this design, a plurality of parallel SMA wires (three or four) are embedded into a flexible multi-lumen tube [183–187, 192]. In all three embodiments of SMA actuated catheters (a)–(c), the actuators are embedded/added in an elongated (pre-loaded) condition and are distributed at an angle of 120°. When the SMA actuator(s) is heated (illustrated in red), it contracts and results in the bending of the distal end towards a specific direction. (d) Conceptual design of a laser-profiled SMA tube (Langelaar *et al*'s design): the distal end consists of laser-cut (or etched) a small diameter SMA tubing. The laser cut patterns facilitate the bending of the distal end in two orthogonal directions. When a specific segment of the tube is locally heated, it contracts, and the distal end bends accordingly [188–191]. In all the four cases illustrated (a)–(d), only two bending directions are shown (for better clarity).

because of the space occupied by the driving fluid. The main strength of magnetic actuation is its ability to 'wirelessly' manipulate catheters without the need for mechanical and fluidic components. On the other hand, the difficulty of achieving precise motions, and the need for customised 'interleaved' MRI sequences to simultaneously visualise and steer catheters continue to remain as challenges for MR-actuated catheters. SMA actuated catheters show great potential for miniaturization as a result of their large power (work) density, i.e. ability to lift more than 100 times its weight. They are, however, inherently nonlinear materials exhibiting significant hysteresis, which makes it difficult to control them in a repeatable manner [196, 197].

3.4.5.2. Safety

Steering without posing any risk to the physiological processes and causing any complications to anatomical structures is crucial for the adoption and commercialisation of deflectable catheters [15]. The two main sources of safety hazards are the steering mechanism or the catheter tracking method. Tendon-driven

Table 5. Actuation techniques summarised based on working principle, steerability and safety.

Actuation [Ref]	Working principle	Steerability	Safety
Tendon(s) [6, 7, 141, 142, 144, 145]	Tendons run from the proximal end through the catheter shaft to the distal end. When the tendon is pushed/pulled, the distal end of the catheter tip is deflected.	+ Swift manipulation − Mechanical nonlinearities which increase with the number of moving parts and DOF − Uncontrollable changes in tendon length due to the passive bending of the catheter shaft while manoeuvring through tortuous anatomies	+ No risk of resistive heating and RF induced heating − (Multi-segment) Sharp or irregular edges may cause damage to the vessel wall
Hydraulic [146–153]	Catheters are controlled by a single or multiple pressurized tube that run to the soft and flexible distal chamber(s). The drive of the hydraulic chamber relies on the pressure of the fluid to cause a bending force in a specific direction.	+ Smooth movement + Precise control of deflectable segments − Slower response time (when compared to tendon driven catheters) − Need for additional equipment such as pumps, valves, and pipes − Possible leakage may limit the catheter's efficiency − Requirements of sophisticated ontrol methods	+ No risk of resistive heating and RF induced heating − If not properly controlled, the pressurised fluid ejected can damage soft tissue
Magnetic [155–165]	Magnetic actuation is based on the changes in magnetic field applied to the distal end of catheters having magnetic or electromagnetic elements.	+ 'Wireless' manipulation without mechanical and fluid components − Difficult to achieve precise motion − Requires customised 'interleaved' MR sequences for simultaneous visualisation and control	**Microcoiled catheter** − Possibility of resistive heating and RF induced heating **Ferromagnetic Spheres** + No risk of resistive heating and RF induced heating − Strong static gradient at the entrance of the MRI bore creates a magnetic force acting on the ferromagnetic element, which can damage the vessel wall
SMAs [178–192]	SMA driven method takes advantage of the shape memory effect of SMA.	+ Great potential for miniaturization − Difficult to be controlled in a repeatable manner due to hysteresis	− Possibility of resistive heating and RF induced heating

catheters, HDCs, and magnetic driven (ferromagnetic spheres) catheters all have the added advantage of not having any long conductive wires, unlike SMA driven catheters, magnetic driven (microcoiled) catheters, and actively tracked catheters. The drawback of having long conductive wires is the risk of resistive heating and RF induced heating. Heating leads to heat stress (inability to control the body's internal temperature), induced current burns and contact burns of body tissues. As summarised by the international commission on Non-Ionising Radiation Protection (ICNIRP): with regards to localised heating, adverse effects can be avoided, if temperatures in localised regions of the head are less than 38 °C, the trunk less than 39 °C, and the limbs less than 40 °C [198]. Typically, the temperature rise is dependent on the balance between the energy absorbed by, and the energy transferred from the region of interest. The factors which play a role in the rate of heat dissipation include the ambient temperature, blood flow, airflow, patient clothing, and humidity [199]. To ameliorate the resistive heating effect, Bernhardt *et al* employed an alumina catheter tip over the initially used polyimide material and by running saline fluid at room temperature through the lumen of the catheter. This approach is similar to current clinical practice in which saline drips are used to reduce the risk of catheter thrombosis, i.e. formation of blood clots [154, 156]. As previously mentioned, Caenazzo *et al* on the other hand, proposed the concept of using conductive fluids to alleviate the effects of heating and artefacts in MR environments [153]. The safety hazard associated with HDCs is the need for high fluidic pressures which, if not controlled properly, may result in jets of pressurized liquid that could damage soft tissue [193, 200]. The safety concern linked to catheters driven by ferromagnetic spheres is the insertion of ferromagnetic components at the entry region of the MRI bore, where a very strong peak static

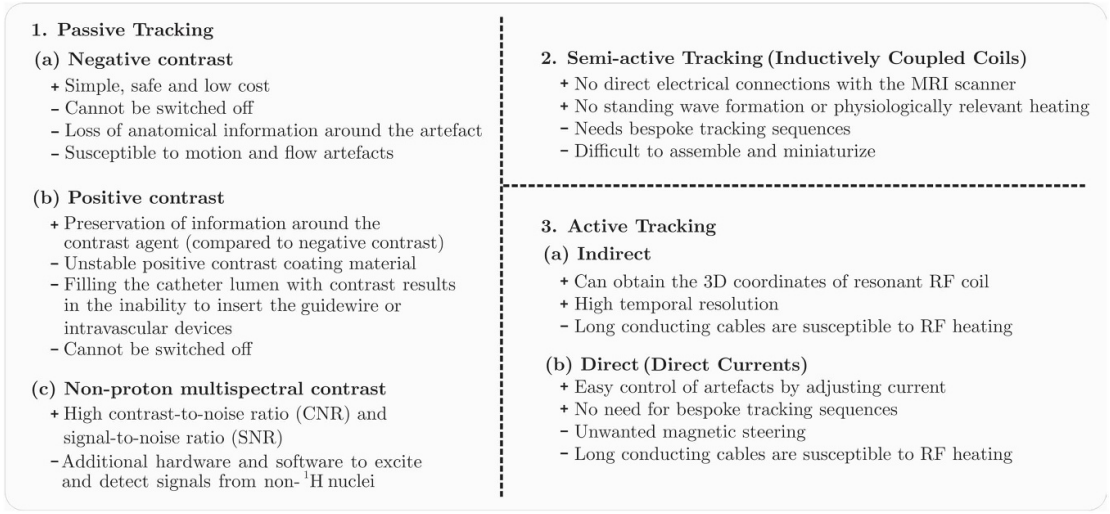

Figure 17. Advantages and disadvantages of tracking methods (marking) for interventional devices.

field gradient of 7.2 T m^{-1} for three Tesla MRI scanners exist [201]. In this region, magnetic forces would be high enough to damage the blood vessel wall [165]. Tendon-driven catheters are generally considered safe; however, catheters with multiple segments should not have any sharp or irregular edges which can damage blood vessel walls and increase the risk of embolisation [15].

3.5. MR visibility

Real-time tracking and visualisation of instruments (guidewires, selective and steerable catheters) in MRI environments are crucial to the success of, and transition to MR-guided endovascular interventions [14]. The restriction on the usage of ferromagnetic materials due to the presence of a strong magnetic field and the difficulty of visualising and localising the relatively safe polymeric materials due to their low magnetic susceptibility [14], has impeded the advancement of MR-guided interventions. In 2001, Duerk *et al* broadly classified catheter tracking methods into passive tracking, semi-active tracking and active tracking (figure 17) [202].

Passive tracking is visualising instruments within MR images either by the materials incorporated in the instrument's construction or by the added markers that enhance, reduce, or distort the T_1- or T_2- weighted MR signals (figure 8 illustrates the definitions of T_1 and T_2). An image is considered T_1-weighted when the signal acquisition parameters are chosen to reflect the variations in T_1 (same applies to T_2-weighted images). Passive markers can be further classified into negative contrast, positive contrast, and non-proton multispectral contrast [136].

In the negative contrast approach, the incorporated materials or added markers make instruments visible by introducing localised magnetic field inhomogeneities which lead to the dephasing of adjacent proton spins and a local signal void (susceptibility artefact) on an MR image [136, 137]. From the previously described steerable catheters, the ones which make use of the negative contrast effect are constructed from the following materials: nitinol hypotubes [141, 142], ferromagnetic spheres [162–165], and SMA wires [192]. In addition to their primary function of providing kink resistance (nitinol hypotubes) and catheter steering (ferromagnetic spheres and SMA wires), these materials produce susceptibility artefacts which make catheters visible on an MR image. Negative contrast passive tracking can also be realised by adding markers to catheters which are not constructed from components that generate susceptibility artefacts. A majority of the previously described guidewires developed for MR-guidance adopt this type of marking for MR visibility; by employing discretely attached or adhered (super) paramagnetic iron oxide (SPIO) nanoparticles [116, 118, 124, 127, 129], iron microparticles embedded in the guidewire's coating [115] and iron microparticles doped in the epoxy resin used in the micropultrusion process of glass or aramid fibres [125]. Simiarly, for steerable catheters, paramagnetic iron oxide (FeO) microparticles were also adhered to the catheter's shaft and distal end in order to create signal voids [7]. Other marker materials include ferromagnetic (e.g. AISI 410 stainless-steel, nickel), ferrimagnetic (e.g. copper zinc ferrite), and strongly paramagnetic (e.g. dysprosium oxide) [136]. Maes *et al* and Miquel *et al* adopted the negative contrast approach by injecting carbon dioxide (CO_2) through a catheter lumen [203] and using balloon catheters inflated with CO_2 [204] respectively. Although the negative contrast approach is relatively simple, safe and low cost, the tracking

cannot be controlled (i.e. switched off), leads to loss of anatomical information around the artefact and is susceptible to motion and flow artefacts [136].

Passive tracking with positive contrast, on the other hand, is achieved by using paramagnetic materials (e.g. gadolinium) that cause shortening of the spin-lattice relaxation (T_1 relaxation time). The shortening of T_1, results in a signal enhancement/bright spot, which enables the visualisation and tracking of the catheter. Omary *et al* and Unal *et al* tested the feasibility of positive contrast tracking by filling the catheter lumen with gadolinium-based contrast [205, 206]. Other research groups employed multi-step processes to coat off-the-shelf catheters with gadolinium-based coatings [207]. Furthermore, when it comes to steerable catheters, Muller *et al* proposed the possibility of adding contrast agents to the driving fluid of HDCs for better catheter visualisation [154]. The positive contrast effect is best visualised on a standard T_1-weighted pulse sequence. Contrary to negative contrast, positive contrast preserves the anatomical information around the marker. However, positive contrast coating materials are unstable, and filling the catheter lumen with contrast agents prevents it from being used for the insertion of guidewires and intravascular catheters.

Instead of solely depending on the presence of hydrogen protons (^{1}H), researchers investigated the simultaneous detection of signals from other nuclei such as fluorine (^{19}F), hyperpolarised carbon (^{13}C), sodium (^{23}Na), and phosphorus (^{31}P). In this case, device visualisation and localisation are achieved by overlaying a second coloured layer of the independent information detected from the additional nuclei to the anatomical details provided by the standard grey-scale (^{1}H) image [208]. Kozerke *et al* filled a balloon catheter with perfluorooctylbromide (PFOB), and extended the imaging capabilities of a standard system to allow for (^{19}F) excitation and signal detection [209]. Similarly, Magnusson *et al* modified an MRI scanner to enable the tracking and visualisation of a catheter filled with hyperpolarised (^{13}C) [210]. The main benefit of using non-proton passive tracking is its ability to provide high contrast-to-noise ratio (CNR) and signal-to-noise ratio (SNR). In terms of limitations, this method requires additional hardware and software to excite and detect signals from non-(^{1}H) nuclei [136].

While passive tracking relies on intrinsic material properties, semi-active tracking uses wireless self-resonant RF circuits as markers to visualise MR invisible catheters [211]. The resonant circuit is triggered/detuned by the MRI scanner using specially designed MRI sequences [80]. The triggering of the circuit induces a magnetic field which dephases the MR-signal and leads to a susceptibility artefact [212]. To adjust the resonance frequency, Weiss *et al* proposed connecting optical fibres to the circuit to illuminate a photodiode placed in parallel to the coil [213]. The challenges of semi-active tracking include the need for bespoke tracking sequences, and difficulties in assembly and miniaturisation due to the optical interface [80]. In terms of strengths, there are no direct electrical connections with the MRI scanner. This, in turn, eliminates the possibility of standing wave formation and subsequent physiologically relevant heating. Note: Some research groups classify semi-active tracking as inductively coupled coils.

Active tracking of catheters can be implemented in two different ways, i.e. indirect active tracking, and direct active tracking. Generally speaking, actively tracked catheters are equipped with receiver resonant RF coils that are electrically connected via coaxial cables to the receiver channel of the MRI scanner in the case of indirect active tracking and to a controllable power source in the case of direct active tracking. In indirect active tracking, the connection to the MRI receiver channel facilitates the determination of the three-dimensional coordinates of the resonant RF coils, which are then superimposed to previously acquired MR images [214]. Although restricted by the number of MR receiver channels, the main advantage of this method is the ability to get accurate and fast position updates, i.e. high temporal resolution [215, 216]. Several research works used indirect active tracking to track their guidewires under MR guidance where by combining a loopless antenna (e.g. coaxial cable, nitinol rod) for shaft visibility with a coil at the distal end for better tip visibility [140, 217, 218]. In [140], Sonmez *et al* added a fibre optic temperature probe to the guidewire's construction to monitor the temperature in real-time and ensure safe operation. Recently, Alipour *et al* who adopted indirect active tracking, proposed attenuating induced currents along long metallic components of guidewires and catheters by employing miniaturised resonant floating RF traps [219].

In direct active tracking, the flow of current through the RF coils is adjusted using the controllable power source, resulting in an adjustable, locally induced magnetic field inhomogeneity (similar to passive and semi-active tracking methods) [214]. The main difference between this active tracking method and passive tracking is the ability to control the generated artefacts interactively during the procedure by simply adjusting the current. When compared to semi-active tracking, which triggers similar coils using the MR scanner, this active tracking method does not require custom MRI sequences to operate. A common problem faced by this type of active tracking is the movement of the catheter due to the magnetically induced forces and torques experienced by the coiled distal end. Nevertheless, Muller *et al* identified this issue as an opportunity to magnetically actuate and visualise catheters simultaneously [154]. The main limitation of active tracking, for both indirect and direct active tracking, is the potential safety hazards imposed by the long conducting coaxial cables that connect the coil and the MRI receiver/power supply [215]. Note: Some

research groups classify direct active tracking as a passive tracking method (referred to as direct current(s)) instead of active tracking because of its close correspondence to passive tracking [10, 136].

4. Current challenges and future directions

Navigation under MRI promotes endovascular interventions with improved safety and efficacy compared to traditional x-ray guided interventions. One of the most significant obstacles to shifting from x-rays to MRI is the lack of MR-compatible instruments [14, 108]. Although much effort has been made in the development of MR-compatible passive instrumentation (section 3.3), steerable instrumentation (section 3.4), and real-time tracking and visualisation of instruments (section 3.5), there are still various challenges that limit the commercialisation of these devices and the popularity of MR-guided interventions. The future development and adaptation of MR-compatible devices necessitate a focused collaborative research effort, which is summarised within the following categories: materials and fabrication schemes, imaging pulse sequence design, robotic control, safety and coordinated interdisciplinary approach. Through the following categorisation, we aim to consolidate the learnings of the previous section and to provide clear guidelines on how to further accelerate research and development in the burgeoning field of MR-guided endovascular interventions.

4.1. Material and fabrication schemes

Metals, with their excellent mechanical properties and mature fabrication methods, are widely used in various medical devices. However, the use of metals in MR environments is restricted due to safety concerns as presented in section 3.4.5. Glass-fibre reinforced polymers (e.g. glass-fibre reinforced PEEK), and high-strength synthetic fibres (e.g. Kevlar®) are commonly used alternatives for MR-guided interventions. Despite their potential, the development of MR safe and visible devices with similar mechanical performance and reliability to those comprising metallic components is challenging, increasing the cost of development and production. Fabrication approaches that allow rapid and low-cost prototyping, such as extrusion and micropultrusion are crucial for accelerating the research around these devices. Manufacturing solutions that offer scalable productivity with high reproducibility are also important factors to consider during the design and development of new medical devices.

4.2. Imaging pulse sequence design

During image-guided endovascular interventions, clinicians rely on the imaging modality—fluoroscopy or MR—to visualise and guide instruments through the vasculature for diagnosis or therapy. In the case of MRI, it combines a high soft tissue contrast, freedom of choosing an imaging plane, and the ability to visualise functional information such as changes in temperature, tissue oxygenation, perfusion, diffusion and flow [10]. For more than a decade, fast imaging pulse sequences with sufficient temporal and spatial resolution for endovascular applications (e.g. vena cava filter placement, stent-graft implantation) have become available for clinical use. However, for other applications (e.g. intracranial applications such as intracerebral coiling), the imaging sequences need to be further improved before clinical translation. Moreover, high spatial resolution often comes with lower temporal resolution. This is a major challenge not only for clinicians looking for high spatial and temporal resolution, but also for devices utilising magnetic fields for simultaneous actuation and visualisation. An important future direction is to find the balance between high feedback rates and information detail by identifying the truly critical feedback information based on the application [166]. For semi-active tracking method as described in section 3.5, which requires bespoke tracking sequences to visualise the device as well as the tissue, similar problems are faced. Regarding other tracking techniques, depending on the marker or antenna material's characteristics, suitable sequences need to be selected or adapted accordingly to control the artefact size and achieve optimum visualisation.

4.3. Robotic control

Robotic surgery is one of the most popular topics in the field of biomedical engineering, and it has become a growing trend by virtue of its great potential. With adequate control, robotic manipulation could improve the precision and accuracy of minimally invasive surgeries (MISs). Of the several actuation modes examined in the article, apart from tendon-driven catheters that can be directly controlled manually, all other types of actuation modes (hydraulic, magnetic and SMA) require varying degrees of remote or automated control. In fluoroscopy-guided endovascular interventions, commercially-available robotic platforms (e.g. CorPath® GRX platform (Corindus, Waltham, MA, USA)) allow surgeons to perform interventions by remotely manipulating off-the-shelf instrumentation from a shielded environment to minimise their exposure to ionising radiations. In MR-guided interventions, robotic surgery can also address issues such as limited access to the patient, which increases the surgeon's risk of developing musculoskeletal injury and escalate medical

errors and risk for the patient [220]. Various acoustic noise types are generated while operating MR systems, most prominently due to the gradient magnetic field. This noise occurs as a result of the rapid alterations of currents within the MR's gradient coils. The problems associated with such noise for interventionalists may include simple annoyance, verbal communication difficulties, heightened anxiety, and hearing impairment [221]. Therefore, it is recommended for both the patients and healthcare workers to wear ear protection, i.e. earplugs or headphones, during interventional MR procedures (as shown in figure 9). Nevertheless, wearing ear protection can also be uncomfortable if worn for an extended period of time. Moreover, to benefit from teleoperation, robotic catheterisation could potentially help overcome these challenges.

Operating a robot under MR-guidance is an active research area that has seen great advancements over the last two decades [222–224]. In addition to the previously mentioned MR safe and MR-conditional robot-assisted platforms for endovascular interventions in section 2.4.3 [79–82], several research groups have investigated other clinical applications such as breast biopsy [225], prostate biopsy [226–228], and stereotactic neurosurgery [229], to name a few. These research developments, especially in MR safe actuation (e.g. pneumatic, hydraulic) have not only help advance MR robotics in their respective clinical fields, but also accelerate research in MR-guided endovascular robotics. One relevant example, is the adoption of the pneumatic stepper motors which were initially developed for actuating a breast biopsy robot [225], in the remote manipulation of off-the-shelf catheters and guidewires [81, 82].

4.4. Safety

The safety of patients and healthcare professionals is the primary consideration in surgical interventions. For MR-guided interventions, the main safety concern is associated with RF-induced and resistive heating caused by the long conductive wires embedded in the instrumentation. Some actuation methods (e.g. SMA actuated catheters), and real-time tracking methods (e.g. active tracking) employ long conductive wires to achieve their desired functionality. Future directions should focus on alleviating the undesirable heating effects through the adoption of novel methods, such as the segmentation of the metal braids [109] or guidewire core [124]. In general, the development of MR safe and MR conditional products that comply with the safety standards set by ASTM F2503 [111] and regulatory bodies (e.g. Food and Drug Administration (FDA)) is crucial for subsequent clinical investigation and commercialisation.

4.5. Coordinate interdisciplinary approach

A system-level approach is highly needed [10]. All these approaches for future directions involve a diverse set of skills from a variety of fields. It is, therefore, difficult to make breakthroughs in MR-guided interventions with individualistic efforts. To advance the progress of endovascular interventions, and to fully exploit the potential of MR in endovascular interventions, there is an urgent need for systematic communication and collaboration among researchers from different backgrounds—engineers, physicists, radiologists, physicians etc. With the synergy of research efforts from various fields, safer medical treatments will become widespread for healthcare professionals and patients.

5. Conclusion

MRI has greatly improved the sensitivity and accuracy of diagnostic imaging. However, for the broader adoption of MRI in interventional radiology and targeted therapy, it is crucial for all the stakeholders involved to collaborate more effectively on overcoming the barriers for safer endovascular treatments. For MR-guided interventions to become part of the clinical routine, the following challenges need to be addressed: high setup and running costs of MRI scanners, lack of MR safe interventional instruments, increased workflow complexity, and access to clinical training in MR environments. Despite these challenges, in recent years, researchers have proven that MRI is safe and practical in a clinical setting [9, 230–232], permits better soft-tissue visualisation, provides more pertinent physiological information (e.g. perfusion MR imaging), and results in no radiation exposure when compared to fluoroscopy-guided procedures. Such clinical endeavours can be further accelerated by supporting on-going research in the fields of MR compatible and visible materials, novel fabrication schemes, dedicated pulse sequence designs, and robotic-assisted surgery. Moreover, companies such as Imricor (electrophysiology mapping and ablation catheters), MaRVis Medical (guidewires), nano4imaging (guidewires), EPFlex (guidewires), and Innovative Tomography Products GmbH (biopsy catheters) are paving the way towards the translation and commercialisation of MR safe and MR conditional devices [13].

In this review, we have presented an illustrative overview of commercially available instrumentation for x-ray fluoroscopy guided interventions. This was followed by an overview of the ongoing and recent developments on navigational instruments for MR-guided interventions. While a number of challenges remain, this review article has sought to highlight the importance of structural and functional materials for

the advancement of multi-functional, easy to use, safe and cost-effective MR safe medical devices. With the pursuit of adopting endovascular interventions under MR-guidance still underway, the following take-home messages outline the requirements to be fulfilled by researchers and companies targeting the development of navigational devices for MRI: (a) MR visible navigational instruments, i.e. clinicians should be able to visualise the instrument's shaft in its entirety, along with the exact tip location as experienced under fluoroscopy. This would significantly speed up the learning curve of clinicians trained on fluoroscopy-guided endovascular interventions. (b) Instruments should have the same mechanical integrity and features as their MR unsafe equivalents. (c) For steerable catheters: development of an intuitive method of controlling the catheter without the need for cumbersome hardware and software [15]. Reducing the complexity of the steerable catheter construction not only simplifies the regulatory process of the medical device, but it also speeds up the clinician's learning curve, reduces the device's cost, and increases the overall reliability and safety of the system. (d) MR safe instrumentation should be made available at a competitive price point when compared to fluoroscopy-guided catheters. This is based on the fact that public healthcare systems would greatly adopt new technologies if they are cost-effective and provide added value in the clinical care of patients. (e) Closely collaborating with clinicians who can identify diseases where MR-guidance can provide a competitive advantage over fluoroscopy-guidance (e.g. ventricular tachycardia [233]).

As our research and understanding of MRI and MR-related technologies move forward, great strides can be made towards improving the quality and safety of patient healthcare.

Data availability statement

The 3D CAD models (Solidworks and STEP files) used in this article are openly available in the figshare repository: https://doi.org/10.6084/m9.figshare.15044136.

Acknowledgment

This work was financially supported by the Engineering and Physical Sciences Research Council (EPSRC), United Kingdom (EP/P012779, Micro-Robotics for Surgery). We would like to acknowledge Dr Lars G Hanson for his input on the MR physics figures and Dr. Wenqiang Chi for his input on the robotic-assisted platforms review.

ORCID iDs

Mohamed E M K Abdelaziz https://orcid.org/0000-0003-2763-8998
Guang-Zhong Yang https://orcid.org/0000-0003-4060-4020
Burak Temelkuran https://orcid.org/0000-0003-2390-5091

References

[1] Kaplan J A, Augoustides J G T, Manecke G R, Maus T and Reich D L 2017 *Kaplan's Cardiac Anesthesia : for Cardiac and Noncardiac Surgery* (Amsterdam: Elsevier)
[2] Venneri L *et al* 2009 Cancer risk from professional exposure in staff working in cardiac catheterization laboratory: Insights from the National Research Council's Biological Effects of Ionizing Radiation VII Report *Am. Heart J.* **157** 118
[3] Rocchini A P and DeWitt A G 2017 *Pediatric Cardiovascular Physiology* (Berlin: Springer) pp 1–17
[4] Nagarajan D V, AlTurki A and Ernst S 2019 *Radiation Exposure and Safety for the Electrophysiologist* (Berlin: Springer) pp 17–28
[5] Roguin A, Goldstein J, Bar O and Goldstein J A 2013 Brain and neck tumors among physicians performing interventional procedures *Am. J. Cardiol.* **111** 1368
[6] Clogenson H C M 2014 MRI-compatible endovascular instruments: improved maneuverability during navigation PhD Thesis Delft University of Technology, Netherlands
[7] Clogenson H C M, van Lith J Y, Dankelman J, Melzer A and van den Dobbelsteen J J 2015 Multi-selective catheter for MR-guided endovascular interventions *Med. Eng. Phys.* **37** 623
[8] Ghatan C E 2020 Understanding and managing occupational radiation exposure for the pregnant interventional radiology nurse *J. Radiol. Nurs.* **39** 20
[9] Razavi R *et al* 2003 Cardiac catheterisation guided by MRI in children and adults with congenital heart disease *Lancet* **362** 1877
[10] Bock M and Wacker F K 2008 MR-guided intravascular interventions: techniques and applications *J. Magn. Reson. Imaging* **27** 326
[11] Kuehne T *et al* 2003 Endovascular stents in pulmonary valve and artery in swine: feasibility study of MR imaging–guided deployment and postinterventional assessment *Radiology* **226** 475
[12] Deng J, Miller F H, Rhee T K, Sato K T, Mulcahy M F, Kulik L M, Salem R, Omary R A and Larson A C 2006 Diffusion-weighted MR imaging for determination of hepatocellular carcinoma response to yttrium-90 radioembolization *J. Vascular Intervent. Radiol.* **17** 1195
[13] Clogenson H and Dobbelsteen J 2016 Catheters and guidewires for interventional MRI: are we there yet? *Imaging Med.* **8** 4
[14] Pushparajah K, Chubb H and Razavi R 2018 MR-guided cardiac interventions *Top. Magn. Reson. Imaging* **27** 115
[15] Ali A, Plettenburg D H and Breedveld P 2016 Steerable catheters in cardiology: classifying steerability and assessing future challenges *IEEE Trans. Biomed. Eng.* **63** 679

[16] Le H M, Do T N and Phee S J 2016 A survey on actuators-driven surgical robots *Sens. Actuators* A **247** 323
[17] Hu X, Chen A, Luo Y, Zhang C and Zhang E 2018 Steerable catheters for minimally invasive surgery: a review and future directions *Comput. Assist. Surg.* **23** 21
[18] da Veiga T, Chandler J H, Lloyd P, Pittiglio G, Wilkinson N J, Hoshiar A K, Harris R A and Valdastri P 2020 Challenges of continuum robots in clinical context: a review *Progr. Biomed. Eng.* **2** 032003
[19] Tóth G G, Yamane M and Heyndrickx G R 2015 How to select a guidewire: technical features and key characteristics *Heart* **101** 645
[20] Buller C 2013 Coronary guidewires for chronic total occlusion procedures: function and design *Intervent. Cardiol.* **5** 533
[21] Gupta V 2019 (Selfex Devices Inc) US20190192828A1
[22] Truckai C 1997 WO9737713A1
[23] Parisi M, Willard M, Wang Y, Bianchi R J and Rubesch T L 2003 (Boston Scientific Scimed Inc) US6648874B2
[24] Opolski M P 2001 (Surface Solutions Laboratories Inc) US6238799B1
[25] Horrigan J B and Riopel M C 1998 (Medtronic Inc) US5792124A
[26] Wang J C 1996 US5533985A
[27] To J T 2009 (Specialized Vascular Technologies Inc) US2009043330A1
[28] Ebnesajjad S 2014 *Fluoroplastics, Volume 1: Non-Melt Processible Fluoropolymers — The Definitive User's Guide and Data Book* 2nd edn (Amsterdam: Elsevier)
[29] Raeder-Devens J E, Shelso S I, Hemerick J F, Schneider E M, Getty H L, Borgmann D M, Sisombath K and Helgerson J A 2013 (Boston Scientific Scimed Inc) US8535369B2
[30] Peterson A A, Logan J B, Patel M R and Polley W F 1998 (Boston Scientific Scimed Inc) US5836926A
[31] Moore P 2005 MRI-guided congenital cardiac catheterization and intervention: the future? *Catheter. Cardiovascular Intervent.* **66** 1
[32] Rothmore P 2002 Lead aprons, radiographers, and discomfort: a pilot study *J. Occupational Health Saf.* **18** 357
[33] Journy N *et al* 2018 Projected future cancer risks in children treated with fluoroscopy-guided cardiac catheterization procedures *Circ.: Cardiovascular Intervent.* **11** e006765
[34] Vandenberghe W and Hoste E 2019 Contrast-associated acute kidney injury: does it really exist, and if so, what to do about it? *F1000Research* **8** 753
[35] Roy K, Gomez-Pulido F and Ernst S 2016 Remote magnetic navigation for catheter ablation in patients with congenital heart disease: a review *J. Cardiovascular Electrophysiol.* **27** S45
[36] Rafii-Tari H, Payne C J and Yang G-Z 2014 Current and emerging robot-assisted endovascular catheterization technologies: a review *Ann. Biomed. Eng.* **42** 697
[37] Antoniou G A, Riga C V, Mayer E K, Cheshire N J and Bicknell C D 2011 Clinical applications of robotic technology in vascular and endovascular surgery *J. Vascular Surg.* **53** 493
[38] Riga C, Bicknell C, Cheshire N and Hamady M 2009 Initial clinical application of a robotically steerable catheter system in endovascular aneurysm repair *J. Endovascular Ther.* **16** 149
[39] Riga C V, Bicknell C D, Rolls A, Cheshire N J and Hamady M S 2013 Robot-assisted fenestrated endovascular aneurysm repair (fevar) using the Magellan system *J. Vascular Interventional Radiol.* **24** 191
[40] Granada J F, Delgado J A, Uribe M P, Fernandez A, Blanco G, Leon M B and Weisz G 2011 First-in-human evaluation of a novel robotic-assisted coronary angioplasty system *JACC: Cardiovascular Intervent.* **4** 460
[41] Al Nooryani A and Aboushokka W 2018 Rotate-on-retract procedural automation for robotic-assisted percutaneous coronary intervention: first clinical experience *Case Rep. Cardiol.* **2018** 6086034
[42] Patel T M, Shah S C and Pancholy S B 2019 Long distance tele-robotic-assisted percutaneous coronary intervention: a report of first-in-human experience *EClinicalMedicine* **14** 53
[43] Saliba W *et al* 2008 Atrial fibrillation ablation using a robotic catheter remote control system: initial human experience and long-term follow-up results *J. Am. College Cardiol.* **51** 2407
[44] Di Biase L *et al* 2009 Ablation of atrial fibrillation utilizing robotic catheter navigation in comparison to manual navigation and ablation: single-center experience *J. Cardiovascular Electrophysiol.* **20** 1328
[45] Knight B, Ayers G M and Cohen T J 2008 Robotic positioning of standard electrophysiology catheters: a novel approach to catheter robotics *J. Invasive Cardiol.* **20** 250
[46] Khan E M *et al* First experience with a novel robotic remote catheter system: Amigo™ mapping trial 2013 *J. Intervent. Cardiac Electrophysiol.* **37** 121
[47] Datino T, Arenal A, Pelliza M, Hernández-Hernández J, Atienza F, González-Torrecilla E, Avila P, Bravo L and Fernández-Avilés F 2014 Comparison of the safety and feasibility of arrhythmia ablation using the Amigo robotic remote catheter system versus manual ablation *Am. J. Cardiol.* **113** 827
[48] López-Gil M *et al* 2014 Cavo-tricuspid isthmus radiofrequency ablation using a novel remote navigation catheter system in patients with typical atrial flutter *Europace* **16** 558
[49] Shaikh Z A, Eilenberg M F and Cohen T J 2017 The Amigo™ remote catheter system: from concept to bedside *J. Innov. Cardiac Rhythm Manage.* **8** 2795
[50] Wutzler A *et al* 2014 Robotic ablation of atrial fibrillation with a new remote catheter system *J. Intervent. Cardiac Electrophysiol.* **40** 215
[51] Ernst S *et al* 2004 Initial experience with remote catheter ablation using a novel magnetic navigation system *Circulation* **109** 1472
[52] Ernst S *et al* 2004 Modulation of the slow pathway in the presence of a persistent left superior caval vein using the novel magnetic navigation system Niobe *EP Europace* **6** 10
[53] Pappone C *et al* 2006 Robotic magnetic navigation for atrial fibrillation ablation *J. Am. College Cardiol.* **47** 1390
[54] Chun J K-R *et al* 2007 Remote-controlled catheter ablation of accessory pathways: results from the magnetic laboratory *Eur. Heart J.* **28** 190
[55] Di Biase L *et al* 2007 Remote magnetic navigation: human experience in pulmonary vein ablation *J. Am. College Cardiol.* **50** 868
[56] Carpi F and Pappone C 2009 Stereotaxis Niobe® magnetic navigation system for endocardial catheter ablation and gastrointestinal capsule endoscopy *Expert Rev. Med. Dev.* **6** 487
[57] Atmakuri S R, Lev E I, Alviar C, Ibarra E, Raizner A E, Solomon S L and Kleiman N S 2006 Initial experience with a magnetic navigation system for percutaneous coronary intervention in complex coronary artery lesions *J. Am. College Cardiol.* **47** 515
[58] Thornton A S and Jordaens L J 2006 Remote magnetic navigation for mapping and ablating right ventricular outflow tract tachycardia *Heart Rhythm* **3** 691

[59] Choi M S, Oh Y-S, Jang S W, Kim J H, Shin W S, Youn H-J, Jung W S, Lee M Y and Seong K B 2011 Comparison of magnetic navigation system and conventional method in catheter ablation of atrial fibrillation: is magnetic navigation system is more effective and safer than conventional method? *Korean Circ. J.* **41** 248
[60] Kiemeneij F, Patterson M S, Amoroso G, Laarman G and Slagboom T 2008 Use of the Stereotaxis Niobe® magnetic navigation system for percutaneous coronary intervention: results from 350 consecutive patients *Catheter. Cardiovascular Intervent.* **71** 510
[61] Armacost M P, Adair J, Munger T, Viswanathan R R, Creighton F M, Curd D T and Sehra R 2007 Accurate and reproducible target navigation with the Stereotaxis Niobe® magnetic navigation system *J. Cardiovascular Electrophysiol.* **18** S26
[62] Gang E S *et al* 2011 Initial animal validation of a new remote electrophysiology catheter guidance and control system *Circ.: Arrhythmia Electrophysiol.* **4** 770
[63] Nguyen B L *et al* 2013 Non-fluoroscopic transseptal catheterization during electrophysiology procedures using a remote magnetic navigation system *J. Atrial Fibrillation* **6** 963
[64] Filgueiras-Rama D, Estrada A, Shachar J, Castrejón S, Doiny D, Ortega M, Gang E and Merino J L 2013 Remote magnetic navigation for accurate, real-time catheter positioning and ablation in cardiac electrophysiology procedures *J. Vis. Exp.* e3658
[65] Yang G-Z *et al* 2017 Medical robotics—regulatory, ethical, and legal considerations for increasing levels of autonomy *Sci. Robot.* **2** eaam8638
[66] Srimathveeravalli G, Kesavadas T and Li X 2010 Design and fabrication of a robotic mechanism for remote steering and positioning of interventional devices *Int. J. Med. Robot. Comput. Assist. Surg.* **6** 160
[67] Wang T, Zhang D and Da L 2010 Remote-controlled vascular interventional surgery robot *Int. J. Med. Robot. Comput. Assist. Surg.* **6** 194
[68] Fu Y, Gao A, Liu H, Li K and Liang Z 2011 Development of a novel robotic catheter system for endovascular minimally invasive surgery *Proc. of The2011 IEEE Int. Conf. on Complex Medical Engineering (Harbin, China)* pp 400–5
[69] Zakaria N A C, Komeda T, Low C Y, Makoto M, Kobayashi M, Ismail A Y and Dumitrescu R 2013 Development of foolproof catheter guide system based on mechatronic design *Prod. Eng.* **7** 81
[70] Sankaran N K, Chembrammel P, Siddiqui A, Snyder K and Kesavadas T 2018 Design and development of surgeon augmented endovascular robotic system *IEEE Trans. Biomed. Eng.* **65** 2483
[71] Feng Z-Q, Bian G-B, Xie X-L, Hou Z-G and Hao J-L 2015 Design and evaluation of a bio-inspired robotic hand for percutaneous coronary intervention *Proc. of The 2015 IEEE Int. Conf. on Robotics and Automation (ICRA) (Seattle, WA, USA)* pp 5338–43
[72] Tavallaei M A, Lavdas M K, Gelman D and Drangova M 2016 Magnetic resonance imaging compatible remote catheter navigation system with 3 degrees of freedom *Int. J. Comput. Assist. Surg.* **11** 1537
[73] Omisore O M, Han S P, Ren L X, Wang G S, Ou F L, Li H and Wang L 2018 Towards characterization and adaptive compensation of backlash in a novel robotic catheter system for cardiovascular interventions *IEEE Trans. Biomed. Circuits Syst.* **12** 824
[74] Thakur Y, Bax J S, Holdsworth D W and Drangova M 2009 Design and performance evaluation of a remote catheter navigation system *IEEE Trans. Biomed. Eng.* **56** 1901
[75] Song Y, Guo S, Zhang L and Yu M 2017 Haptic feedback in robot-assisted endovascular catheterization *Proc. of The2017 IEEE Int. Conf. on Mechatronics and Automation (ICMA) (Takamatsu, Japan)* pp 404–9
[76] Bian G, Xie X, Feng Z, Hou Z, Wei P, Cheng L and Tan M 2013 An enhanced dual-finger robotic Hand for Catheter manipulating in vascular intervention: a preliminary study *Proc. of The2013 IEEE Int. Conf. on Information and Automation(ICIA) (Yinchuan, China)* pp 356–61
[77] Guo S, Qin M, Xiao N, Wang Y, Peng W and Bao X 2016 High precise haptic device for the robotic catheter navigation system *Proc. of The 2016 IEEE Int. Conf. on Mechatronics and Automation(ICMA) (Harbin, China)* pp 2524–29
[78] Wang K, Chen B, Lu Q, Li H, Liu M, Shen Y and Xu Z 2018 Design and performance evaluation of real-time endovascular interventional surgical robotic system with high accuracy *Int. J. Med. Robot. Comput. Assist. Surg.* **14** e1915
[79] Tavallaei M A, Thakur Y, Haider S and Drangova M 2013 A magnetic-resonance-imaging-compatible remote catheter navigation system *IEEE Trans. Biomed. Eng.* **60** 899
[80] Lee K, Fu K C D, Guo Z, Dong Z, Leong M C W, Cheung C, Lee A P, Luk W and Kwok K 2018 MR safe robotic manipulator for MRI-guided intracardiac catheterization *IEEE/ASME Trans. Mechatronics* **23** 586
[81] Abdelaziz M E M K *et al* 2019 Toward a versatile robotic platform for fluoroscopy and MRI-guided endovascular interventions: a pre-clinical study *Proc. of The 2019 IEEE/RSJ Int. Conf. on Intelligent Robots and Systems (IROS)* (*Macau, China*) pp 5411–18
[82] Kundrat D, Dagnino G, Kwok T M Y, Abdelaziz M E M K, Chi W, Nguyen A, Riga C V and Yang G-Z 2021 An MR-safe endovascular robotic platform: design, control, and ex-vivo evaluation *IEEE Trans. Biomed. Eng.* 1–1
[83] Chi Wenqiang 2019 Context-aware learning for robot-assisted endovascular catheterization PhD Thesis Imperial College London, United Kingdom
[84] Hwang J, Kim J-Y and Choi H 2020 A review of magnetic actuation systems and magnetically actuated guidewire- and catheter-based microrobots for vascular interventions *Intell. Serv. Robot.* **13** 1
[85] Piorkowski C *et al* 2008 Steerable sheath catheter navigation for ablation of atrial fibrillation: a case-control study *Pacing Clin. Electrophysiol.* **31** 863
[86] Matsuo S *et al* 2010 Prospective randomized comparison of a steerable versus a non-steerable sheath for typical atrial flutter ablation *EP Europace* **12** 402
[87] Piorkowski C *et al* 2011 Steerable versus nonsteerable sheath technology in atrial fibrillation ablation: a prospective, randomized study *Circ.: Arrhythmia Electrophysiol.* **4** 157
[88] Matsuo S *et al* 2011 Completion of mitral isthmus ablation using a steerable sheath: prospective randomized comparison with a nonsteerable sheath *J. Cardiovascular Electrophysiol.* **22** 1331
[89] Heidt T *et al* 2019 Real-time magnetic resonance imaging – guided coronary intervention in a porcine model *Sci. Rep.* **9** 8663
[90] Jolesz F A and Blumenfeld S M 1994 *Magn. Reson. Q.* **10** 85
[91] Lufkin R B 1995 Interventional MR imaging *Radiology* **197** 16
[92] Rogers T, Ratnayaka K and Lederman R J 2014 MRI catheterization in cardiopulmonary disease *Chest* **145** 30
[93] Rogers T and Lederman R J 2015 Interventional CMR: clinical applications and future directions *Curr. Cardiol. Rep.* **17** 31
[94] Hanson L G 2008 Is quantum mechanics necessary for understanding magnetic resonance? *Concepts Magnet. Reson.* A **32A** 329
[95] Brown R W, Cheng Y N, Haacke E M, Thompson M R and Venkatesan R 2014 *Magnetic Resonance Imaging: Physical Principles and Sequence Design* 2nd edn (Hoboken: Wiley Inc.)
[96] Plewes D B and Kucharczyk W 2012 Physics of MRI: a primer *J. Magn. Reson. Imaging* **35** 1038
[97] Elster A D and Burdette J H 2001 *Questions & Answers in Magnetic Resonance Imaging* 2nd edn (MO: Mosby, Maryland Heights)

[98] Mahnken A H, Wilhelm K E and Ricke J 2013 *CT- and MR-Guided Interventions in Radiology* (Berlin: Springer)
[99] Thomsen H S 2006 Nephrogenic systemic fibrosis: a serious late adverse reaction to gadodiamide *Eur. Radiol.* **16** 2619
[100] Kos S *et al* 2009 MR-compatible polyetheretherketone-based guide wire assisting MR-guided stenting of iliac and supraaortic arteries in swine: feasibility study *Minimally Invasive Ther. Allied Technol.* **18** 181
[101] Rogers T, Ratnayaka K, Karmarkar P, Campbell-Washburn A E, Schenke W H, Mazal J R, Kocaturk O, Faranesh A Z and Lederman R J 2016 Real-time magnetic resonance imaging guidance improves the diagnostic yield of endomyocardial biopsy *JACC: Basic Transl. Sci.* **1** 376
[102] Phutheho M 2020 Estimation of the eye lens doses in a catheterization laboratory from available image parameters PhD Thesis University of the Free State, South Africa ,
[103] Danias P G, Roussakis A and Ioannidis J P 2004 Diagnostic performance of coronary magnetic resonance angiography as compared against conventional x-ray angiography: a meta-analysis *J. Am. College Cardiol.* **44** 1867
[104] Uecker M, Zhang S, Voit D, Karaus A, Merboldt K-D and Frahm J 2010 Real-time MRI at a resolution of 20 ms *NMR Biomed.* **23** 986
[105] Quick H H, Kuehl H, Kaiser G, Hornscheidt D, Mikolajczyk K P, Aker S, Debatin J F and Ladd M E 2003 Interventional MRA using actively visualized catheters, TrueFISP, and real-time image fusion *Magn. Reson. Med.* **49** 129
[106] Kaul M, Stork A, Bansmann P, Nolte-Ernsting C, Lund G, Weber C and Adam G 2004 *RöFo-Fortschritte auf dem Gebiet der RöNtgenstrahlen und der Bildgebenden Verfahren* (*New York*) vol 176 (© Georg Thieme Verlag KG Stuttgart) pp 1560–5
[107] Ozturk C, Guttman M, McVeigh E R and Lederman R J 2005 Magnetic resonance imaging-guided vascular interventions *Top. Magn. Reson. Imaging: TMRI* **16** 369
[108] Mukherjee R K, Chubb H, Roujol S, Razavi R and O'Neill M D 2019 Advances in real-time MRI–guided electrophysiology *Curr. Cardiovascular Imaging Rep.* **12** 6
[109] Yildirim K D, Basar B, Campbell-Washburn A E, Herzka D A, Kocaturk O and Lederman R J 2019 A cardiovascular magnetic resonance (CMR) safe metal braided catheter design for interventional CMR at 1.5 T: freedom from radiofrequency induced heating and preserved mechanical performance *J. Cardiovascular Magn. Reson.* **21** 16
[110] Abu Hazeem A A, Dori Y, Whitehead K K, Harris M A, Fogel M A, Gillespie M J, Rome J J and Glatz A C 2014 X-ray magnetic resonance fusion modality may reduce radiation exposure and contrast dose in diagnostic cardiac catheterization of congenital heart disease *Catheter. Cardiovascular Intervent.* **84** 795
[111] ASTM F2503-20 Standard Practice for Marking Medical Devices and Other Items for Safety in the Magnetic Resonance Environment 2020 *Report*
[112] Elmar S, Alexander R, Tobias S, Manning Warren J, Günther Rolf W and Arno B 2002 Magnetic resonance–guided coronary artery stent placement in a swine model *Circulation* **105** 874
[113] Elgort D R, Hillenbrand C M, Zhang S, Wong E Y, Rafie S, Lewin J S and Duerk J L 2006 Image-guided and -monitored renal artery stenting using only MRI *J. Magn. Reson. Imaging* **23** 619
[114] Buecker A, Spuentrup E, Schmitz-Rode T, Kinzel S, Pfeffer J, Hohl C, van Vaals J J and Günther R W 2004 Use of a nonmetallic guide wire for magnetic resonance-guided coronary artery catheterization *Investigative Radiol.* **39** 656
[115] Mekle R, Hofmann E, Scheffler K and Bilecen D 2006 A polymer-based MR-compatible guidewire: a study to explore new prospects for interventional peripheral magnetic resonance angiography (ipMRA) *J. Magn. Reson. Imaging* **23** 145
[116] Clogenson H C M, Dankelman J and van den Dobbelsteen J J 2014 Steerable guidewire for magnetic resonance guided endovascular interventions *J. Med. Devices* **8** 021002–1
[117] Bakker C J, Smits H F, Bos C, van der Weide R, Zuiderveld K J, van Vaals J J, Hurtak W F, Viergever M A and Mali W P 1998 MR-guided balloon angioplasty: in vitro demonstration of the potential of MRI for guiding, monitoring, and evaluating endovascular interventions *J. Magn. Reson. Imaging: JMRI* **8** 245
[118] Kos S *et al* 2009 Feasibility of real-time magnetic resonance-guided angioplasty and stenting of renal arteries in vitro and in swine, using a new polyetheretherketone-based magnetic resonance-compatible guidewire. *Investigative Radiol.* **44** 234
[119] Krueger S *et al* 2008 An MR guidewire based on micropultruded fiber-reinforced material *Magn. Reson. Med.* **60** 1190
[120] Aphrodite T *et al* 2010 Magnetic resonance-guided cardiac interventions using magnetic resonance-compatible devices: a preclinical study and first-in-man congenital interventions *Circ.: Cardiovascular Intervent.* **3** 585
[121] Kos S *et al* 2009 First magnetic resonance imaging-guided aortic stenting and cava filter placement using a polyetheretherketone-based magnetic resonance imaging-compatible guidewire in swine: proof of concept *CardioVascular Intervent. Radiol.* **32** 514
[122] Krämer N A *et al* 2009 Preclinical evaluation of a novel fiber compound MR guidewire in vivo *Investigative Radiol.* **44** 390
[123] Pushparajah K, Tzifa A and Razavi R 2014 Cardiac MRI catheterization: a 10-year single institution experience and review *Interventional Cardiol.* **6** 335
[124] Basar B *et al* 2015 Segmented nitinol guidewires with stiffness-matched connectors for cardiovascular magnetic resonance catheterization: preserved mechanical performance and freedom from heating *J. Cardiovascular Magn. Reson.* **17** 105
[125] Klaus Düring J G P 2017 (Marvis Interventional GmbH) US20170232158A1
[126] Massmann A, Buecker A and Schneider G K 2017 Glass-fiber–based MR-safe guidewire for MR imaging–guided endovascular interventions: in vitro and preclinical in vivo feasibility study *Radiology* **284** 541
[127] Wolska-Krawczyk M, Rube M A, Immel E, Melzer A and Buecker A 2014 Heating and safety of a new MR-compatible guidewire prototype versus a standard nitinol guidewire *Radiol. Phys. Technol.* **7** 95
[128] Wolska-Krawczyk M 2013 Evaluation of liver tumor perfusion by intraarterial transcatheter magnetic resonance angiography during transarterial chemoembolization in patients with hepatocellular carcinoma: preclinical instrument validation in vascular models and clinical study PhD Thesis Saarland University, Germany
[129] Brecher C, Emonts M, Brack A, Wasiak C, Schütte A, Krämer N and Bruhn R 2014 New concepts and materials for the manufacturing of MR-compatible guide wires *Biomed. Eng. / Biomed. Tech.* **59** 147
[130] Van de Velde K and Kiekens P 2001 Thermoplastic pultrusion of natural fibre reinforced composites *Compos. Struct.* **54** 355
[131] Veeram Reddy S R *et al* 2020 Invasive cardiovascular magnetic resonance (iCMR) for diagnostic right and left heart catheterization using an MR-conditional guidewire and passive visualization in congenital heart disease *J. Cardiovascular Magn. Reson.* **22** 20
[132] Rube M A, Fernandez-Gutierrez F, Cox B F, Holbrook A B, Houston J G, White R D, McLeod H, Fatahi M and Melzer A 2015 Preclinical feasibility of a technology framework for MRI-guided iliac angioplasty *Int. J. Computer Assist. Radiol. Surg.* **10** 637

[133] Bietenbeck M, Florian A, Chatzantonis G, Meier C, Korthals D, Martens S and Yilmaz A 2019 Introduction of a CMR-conditional cardiac phantom simulating cardiac anatomy and function and enabling training of interventional CMR procedures *Sci. Rep.* **9** 19852
[134] Williams J C 2019 Evaluating EPflex MRline guidewire for endovascular interventions guided by MRI at 3T vs. X-ray fluoroscopy Msc Thesis University of California, USA
[135] Knight D S, Kotecha T, Martinez-Naharro A, Brown J T, Bertelli M, Fontana M, Muthurangu V and Coghlan J G 2019 Cardiovascular magnetic resonance-guided right heart catheterization in a conventional CMR environment – predictors of procedure success and duration in pulmonary artery hypertension *J. Cardiovascular Magn. Reson.* **21** 57
[136] Settecase F, Martin A J, Lillaney P, Losey A and Hetts S W 2015 Magnetic resonance–guided passive catheter tracking for endovascular therapy *Magn. Reson. Imaging Clin. North Am.* **23** 591
[137] Schenck J F 1996 The role of magnetic susceptibility in magnetic resonance imaging: MRI magnetic compatibility of the first and second kinds *Med. Phys.* **23** 815
[138] Li X, Perotti L E, Martinez J A, Duarte-Vogel S M, Ennis D B and Wu H H 2020 Real-time 3T MRI-guided cardiovascular catheterization in a porcine model using a glass-fiber epoxy-based guidewire *PLoS One* **15** e0229711
[139] Carey J, Fahim A and Munro M 2004 Design of braided composite cardiovascular catheters based on required axial, flexural, and torsional rigidities *J. Biomed. Mater. Res.* B **70B** 73
[140] Sonmez M, Saikus C E, Bell J A, Franson D N, Halabi M, Faranesh A Z, Ozturk C, Lederman R J and Kocaturk O 2012 MRI active guidewire with an embedded temperature probe and providing a distinct tip signal to enhance clinical safety *J. Cardiovascular Magn. Reson.* **14** 38
[141] Bell J A, Saikus C E, Ratnayaka K, Wu V, Sonmez M, Faranesh A Z, Colyer J H, Lederman R J and Kocaturk O 2012 A deflectable guiding catheter for real-time MRI-guided interventions *J. Magn. Reson. Imaging* **35** 908
[142] Yao W, Schaeffter T, Seneviratne L and Althoefer K 2012 Developing an magnetic resonance-compatible catheter for cardiac catheterization *J. Med. Dev.* **6** 041002
[143] Dupont P E, Lock J, Itkowitz B and Butler E 2010 Design and Control of Concentric-Tube Robots *IEEE Trans. Robot.* **26** 209
[144] Ataollahi A, Karim R, Fallah A S, Rhode K, Razavi R, Seneviratne L D, Schaeffter T and Althoefer K 2016 Three-degree-of-freedom MR-compatible multisegment cardiac catheter steering mechanism *IEEE Trans. Biomed. Eng.* **63** 2425
[145] Ataollahi A, Althoefer K, Schaeffter T R and Rhode K 2017 (King's College London) US9675781B2
[146] Haga Y, Muyari Y, Mineta T, Matsunaga T, Akahori H and Esashi M 2005 Small diameter hydraulic active bending catheter using laser processed super elastic alloy and silicone rubber tube *Proc. of The 2005 IEEE/EMBS Special Conf. on Microtechnology in Medicine and Biology* (*Oahu, HI, USA*) pp 245–8
[147] Ikuta K, Ichikawa H, Suzuki K and Yamamoto T 2003 Safety active catheter with multi-segments driven by innovative hydro-pressure micro actuators *Proc. of The Sixteenth Annual Int. Conf. on Micro Electro Mechanical Systems* (*Kyoto, Japan*) pp 130–5
[148] Ikuta K, Ichikawa H, Suzuki K and Yajima D 2006 Multi-degree of freedom hydraulic pressure driven safety active catheter *Proc. of The 2006 IEEE Int. Conf. on Robotics and Automation (ICRA)* (*Orlando, FL, USA*) pp 4161–6
[149] Ikuta K, Matsuda Y, Yajima D and Ota Y 2010 Precise bending angle control of hydraulic active catheter by pressure pulse drive *Proc. of The 2010 IEEE Int. Conf. on Robotics and Automation (ICRA)* (*Anchorage, Alaska*) pp 5588–93
[150] De Boer J 2007 (Cordis Corp) US2007060997A1
[151] Johansen J A, Yee C E and Neet J M 2005 (Spectranetics Corp) US6951554B2
[152] Skerven G J 2010 (Cook Endoscopy) US20100168665A1
[153] Caenazzo A and Althoefer K 2018 Hypertonic saline solution for signal transmission and steering in MRI-guided intravascular catheterisation *Proc. of The 2018 TAROS: 19th Conf. Towards Autonomous Robotic Systems* (*Bristol, UK*) pp 284–90
[154] Muller L, Saeed M, Wilson M W and Hetts S W 2012 Remote control catheter navigation: options for guidance under MRI *J. Cardiovascular Magn. Reson.* **14** 33
[155] Roberts T, Hassenzahl W, Hetts S and Arenson R 2002 Remote control of catheter tip deflection: an opportunity for interventional MRI *Magn. Reson. Med.* **48** 1091
[156] Bernhardt A *et al* 2011 Steerable catheter microcoils for interventional MRI: reducing resistive heating *Acad. Radiol.* **18** 270
[157] Malba V, Maxwell R, Evans L B, Bernhardt A F, Cosman M and Yan K 2003 Laser-lathe lithography—a novel method for manufacturing nuclear magnetic resonance microcoils *Biomed. Microdevices* **5** 21
[158] Moftakhar P *et al* 2015 New-generation laser-lithographed dual-axis magnetically assisted remote-controlled endovascular catheter for interventional mr imaging: in vitro multiplanar navigation at 1.5 T and 3 T versus x-ray fluoroscopy *Radiology* **277** 842
[159] Lillaney P V *et al* 2016 Endovascular MR-guided renal embolization by using a magnetically assisted remote-controlled catheter system *Radiology* **281** 219
[160] Liu T, Lombard Poirot N, Greigarn T and Cenk Çavuşoğlu M 2017 Modeling and validation of the three-dimensional deflection of an MRI-compatible magnetically actuated steerable catheter *J. Med. Dev.* **11** 2142
[161] Greigarn T, Poirot N L, Xu X and Çavuşoğlu M C 2019 Jacobian-based task-space motion planning for MRI-actuated continuum robots *IEEE Robot. Autom. Lett.* **4** 145
[162] Mathieu J B, Soulez G, Beaudoin G, Felfoul O, Chanu A and Martel S 2008 Abstract No. 76: steering and tracking of magnetic catheters using MRI systems *J. Vascular Intervent. Radiol.* **19** S31
[163] Lalande V, Gosselin F P and Martel S 2010 Catheter steering using a Magnetic Resonance Imaging system *Proc. of The 2010 Annual Int. Conf. of the IEEE Engineering in Medicine and Biology* (*Buenos Aires, Argentina*) pp 1874–7
[164] Gosselin F P, Lalande V and Martel S 2011 Characterization of the deflections of a catheter steered using a magnetic resonance imaging system *Med. Phys.* **38** 4994
[165] Zhang K, Krafft A J, Umathum R, Maier F, Semmler W and Bock M 2010 Real-time MR navigation and localization of an intravascular catheter with ferromagnetic components *Magn. Reson. Mater. Phys. Biol. Med.* **23** 153
[166] Erin O, Boyvat M, Tiryaki M E, Phelan M and Sitti M 2020 Magnetic resonance imaging system–driven medical robotics *Adv. Intell. Syst.* **2** 1900110
[167] Erin O, Giltinan J, Tsai L and Sitti M 2017 Design and actuation of a magnetic millirobot under a constant unidirectional magnetic field *Proc. of The 2017IEEE Int. Conf. on Robotics and Automation (ICRA)* (*Singapore*) pp 3404–10
[168] Erin O, Gilbert H B, Tabak A F and Sitti M 2019 Elevation and azimuth rotational actuation of an untethered millirobot by MRI gradient coils *IEEE Trans. Robotics* **35** 1323

[169] Folio D, Dahmen C, Wortmann T, Zeeshan M A, Shou K, Pané S, Nelson B J, Ferreira A and Fatikow S 2011 MRI magnetic signature imaging, tracking and navigation for targeted micro/nano-capsule therapeutics (*San Francisco, CA, USA) Proc. of The 2011 IEEE/RSJ Int. Conf. on Intelligent Robots and Systems (IROS)* pp 1297–303
[170] Dahmen C, Belharet K, Folio D, Ferreira A and Fatikow S 2016 MRI-based dynamic tracking of an untethered ferromagnetic microcapsule navigating in liquid *Int. J. Optomechatronics* **10** 73
[171] Mathieu J B and Martel S 2010 Steering of aggregating magnetic microparticles using propulsion gradients coils in an MRI Scanner *Magn. Reson. Med.* **63** 1336
[172] Pouponneau P, Leroux J C and Martel S 2009 Magnetic nanoparticles encapsulated into biodegradable microparticles steered with an upgraded magnetic resonance imaging system for tumor chemoembolization *Biomaterials* **30** 6327
[173] Bigot A, Tremblay C, Soulez G and Martel S 2014 Magnetic resonance navigation of a bead inside a three-bifurcation pmma phantom using an imaging gradient coil insert *IEEE Trans. Robot.* **30** 719
[174] Latulippe M and Martel S 2014 Dipole field navigation for targeted drug delivery *Proc. of The 2014 IEEE RAS and EMBS Int. Conf. on Biomedical Robotics and Biomechatronics* (*São Paulo, Brazil)* pp 320–5
[175] Latulippe M and Martel S 2015 Dipole field navigation: theory and proof of concept *IEEE Trans. Robot.* **31** 1353
[176] Becker A T, Felfoul O and Dupont P E 2015 Toward tissue penetration by MRI-powered millirobots using a self-assembled Gauss gun *Proc. of The 2015 IEEE Int. Conf. on Robotics and Automation (ICRA)* (*Seattle, WA, USA)* pp 1184–89
[177] Wilkes K E, Liaw P K and Wilkes K E 2000 The fatigue behavior of shape-memory alloys *JOM* **52** 45
[178] Lim G, Park K, Sugihara M, Minami K and Esashi M 1996 Future of active catheters *Sens. Actuators* A **56** 113
[179] Fu Y, Li X, Wang S, Liu H and Liang Z 2008 Research on the axis shape of an active catheter *Int. J. Med. Robot. Comput. Assist. Surg.* **4** 69
[180] Chang J K *et al* 2002 Development of endovascular microtools *J. Micromech. Microeng.* **12** 824
[181] Mineta T, Mitsui T, Watanabe Y, Kobayashi S, Haga Y and Esashi M 2001 Batch fabricated flat meandering shape memory alloy actuator for active catheter *Sens. Actuators* A **88** 112
[182] Namazu T, Komatsubara M, Nagasawa H, Miki T, Tsurui T and Inoue S 2011 Titanium-nickel shape memory alloy spring actuator for forward-looking active catheter *J. Metall.* **2011** 685429
[183] Fukuda T, Shuxiang G, Kosuge K, Arai F, Negoro M and Nakabayashi K 1994 Micro active catheter system with multi degrees of freedom *Proc. of The 1994 IEEE Int. Conf. on Robotics and Automation (ICRA)* (*San Diego, CA, USA*) pp 2290–5
[184] Takizawa H, Tosaka H, Ohta R, Kaneko S and Ueda Y 1999 Development of a microfine active bending catheter equipped with MIF tactile sensors *Proc. of The Twelfth IEEE Int. Conf. on Micro Electro Mechanical Systems* (*Orlando, FL, USA)* pp 412–17
[185] Crews J H and Buckner G D 2012 Design optimization of a shape memory alloy–actuated robotic catheter *J. Intell. Mater. Syst. Struct.* **23** 545
[186] Couture T and Szewczyk J 2017 Design and experimental validation of an active catheter for endovascular navigation *J. Med. Dev.* **12** 011003–1
[187] Wiest J H and Buckner G D 2015 Path optimization and control of a shape memory alloy actuated catheter for endocardial radiofrequency ablation *Robot. Auton. Syst.* **65** 88
[188] Langelaar M and van Keulen F 2004 Modeling of a shape memory alloy active catheter *Proc. of The 45th AIAA/ASME/ASCE/AHS/ASC Structures, Structural Dynamics & Conf* (*Palm Springs, California* AIAA 2004-1653)
[189] Langelaar M, Yoon G H, Gurav S, Kim Y Y and Keulen F V 2005 Modeling and design of shape memory alloy actuators *Proc. of the 6th Int. Conf. on Thermal, Mechanial and Multi-Physics Simulation and Experiments in Micro-Electronics and Micro-Systems* (*Berlin, Germany)* pp 626–33
[190] Langelaar M and van Keulen F 2007 Gradient-based design optimization of shape memory alloy active catheters *Proc. of The 48th AIAA/ASME/ASCE/AHS/ASC Structures, Structural Dynamics & Conf.* (*Honolulu, Hawaii*) AIAA 2007-1744
[191] Tung A T, Park B-H, Liang D H and Niemeyer G 2008 Laser-machined shape memory alloy sensors for position feedback in active catheters *Sens. Actuators* A **147** 83
[192] Sheng J, Wang X, Dickfeld T L and Desai J P 2018 Towards the development of a steerable and mri-compatible cardiac catheter for atrial fibrillation treatment *IEEE Robot. Automat. Lett.* **3** 4038
[193] Runciman M, Darzi A and Mylonas G P 2019 Soft robotics in minimally invasive surgery *Soft Robot.* **6** 423
[194] De Greef A, Lambert P and Delchambre A 2009 Towards flexible medical instruments: review of flexible fluidic actuators *Precis. Eng.* **33** 311
[195] Bertetto A M and Ruggiu M 2004 A novel fluidic bellows manipulator *J. Robot. Mechatronics* **16** 604
[196] Mohd Jani J, Leary M, Subic A and Gibson M A 2014 A review of shape memory alloy research, applications and opportunities *Mater. Des. (1980-2015)* **56** 1078
[197] Selden B, Cho K and Asada H H 2006 Segmented shape memory alloy actuators using hysteresis loop control *Smart Mater. Struct.* **15** 642
[198] The Int. Commission on Non-Ionizing Radiation, Protection 2009 ICNIRP statement on the "Guidelines for limiting exposure to time-varying electric, magnetic, and electromagnetic fields (up to 300 GHz)" *Health Phys.* **97** 257
[199] Shellock F G 2000 Radiofrequency energy-induced heating during MR procedures: a review *J. Magn. Reson. Imaging* **12** 30
[200] Le H M, Do T N and Phee S J 2016 A survey on actuators-driven surgical robots *Sens. Actuators* A **247** 323
[201] Shellock F G, Kanal E and Gilk T B 2011 Regarding the value reported for the term "spatial gradient magnetic field" and how this information is applied to labeling of medical implants and devices *Am. J. Roentgenol.* **196** 142
[202] Duerk J L, Wong E Y and Lewin J S 2001 A brief review of hardware for catheter tracking in magnetic resonance imaging *Magn. Reson. Mater. Phys. Biol. Med.* **13** 199
[203] Maes R M, Lewin J S, Duerk J L and Wacker F K 2005 Combined use of the intravascular blood-pool agent, gadomer, and carbon dioxide: A novel type of double-contrast magnetic resonance angiography (MRA) *J. Magn. Reson. Imaging* **21** 645
[204] Miquel M E, Hegde S, Muthurangu V, Corcoran B J, Keevil S F, Hill D L G and Razavi R S 2004 Visualization and tracking of an inflatable balloon catheter using SSFP in a flow phantom and in the heart and great vessels of patients *Magn. Reson. Med.* **51** 988
[205] Omary R A, Unal O, Koscielski D S, Frayne R, Korosec F R, Mistretta C A, Strother C M and Grist T M 2000 Real-time MR imaging-guided passive catheter tracking with use of gadolinium-filled catheters *J. Vascular Intervent. Radiol.* **11** 1079
[206] Unal O, Korosec F R, Frayne R, Strother C M and Mistretta C A 1998 A rapid 2D time-resolved variable-rate k-space sampling MR technique for passive catheter tracking during endovascular procedures *Magn. Reson. Med.* **40** 356
[207] Unal O, Li J, Cheng W, Yu H and Strother C M 2006 MR-visible coatings for endovascular device visualization *J. Magn. Reson. Imaging* **23** 763

[208] Tirotta I, Dichiarante V, Pigliacelli C, Cavallo G, Terraneo G, Bombelli F B, Metrangolo P and Resnati G 2015 ^{19}F magnetic resonance imaging (MRI): from design of materials to clinical applications *Chem. Rev.* **115** 1106
[209] Kozerke S, Hegde S, Schaeffter T, Lamerichs R, Razavi R and Hill D L 2004 Catheter tracking and visualization using ^{19}F nuclear magnetic resonance *Magn. Reson. Med.* **52** 693
[210] Magnusson P, Johansson E, Månsson S, Petersson J S, Chai C-M, Hansson G, Axelsson O and Golman K 2007 Passive catheter tracking during interventional MRI using hyperpolarized ^{13}C *Magn. Reson. Med.* **57** 1140
[211] Kuehne T, Weiss S, Brinkert F, Weil J, Yilmaz S, Schmitt B, Ewert P, Lange P and Gutberlet M 2004 Catheter visualization with resonant markers at MR imaging–guided deployment of endovascular stents in swine *Radiology* **233** 774
[212] Felfoul O, Mathieu J, Beaudoin G and Martel S 2008 In vivo MR-tracking based on magnetic signature selective excitation *IEEE Trans. Med. Imaging* **27** 28
[213] Weiss S, Kuehne T, Brinkert F, Krombach G, Katoh M, Schaeffter T, Guenther R W and Buecker A 2004 In vivo safe catheter visualization and slice tracking using an optically detunable resonant marker *Magn. Reson. Med.* **52** 860
[214] Glowinski A, Adam G, Bücker A, Neuerburg J, van Vaals J J and Günther R W 1997 Catheter visualization using locally induced, actively controlled field inhomogeneities *Magn. Reson. Med.* **38** 253
[215] Xiao X, Huang Z, Rube M A and Melzer A 2017 Investigation of active tracking for robotic arm assisted magnetic resonance guided focused ultrasound ablation *Int. J. Med. Robot. Comput. Assist. Surg.* **13** e1768
[216] Bartels L W and Bakker C J G 2003 Endovascular interventional magnetic resonance imaging *Phys. Med. Biol.* **48** R37
[217] Serfaty J-M, Yang X, Aksit P, Quick H H, Solaiyappan M and Atalar E 2000 Toward MRI-guided coronary catheterization: visualization of guiding catheters, guidewires, and anatomy in real time *J. Magn. Reson. Imaging* **12** 590
[218] Kocaturk O, Kim A H, Saikus C E, Guttman M A, Faranesh A Z, Ozturk C and Lederman R J 2009 Active two-channel 0.035″ guidewire for interventional cardiovascular MRI *J. Magn. Reson. Imaging* **30** 461
[219] Alipour A *et al* 2020 MRI conditional actively tracked metallic electrophysiology catheters and guidewires with miniature tethered radio-frequency traps: theory, design, and validation *IEEE Trans. Biomed. Eng.* **67** 1616
[220] Fernández Gutiérrez F *et al* 2015 Comparative ergonomic workflow and user experience analysis of MRI versus fluoroscopy-guided vascular interventions: an iliac angioplasty exemplar case study *Int. J. Comput. Assist. Radiol. Surg.* **10** 1639
[221] McJury M and Shellock F G 2000 Auditory noise associated with MR procedures: a review *J. Magn. Reson. Imaging* **12** 37
[222] Xiao Q, Monfaredi R, Musa M, Cleary K and Chen Y 2020 MR-conditional actuations: a review *Ann. Biomed. Eng.* **48** 2707
[223] Fisher T, Hamed A, Vartholomeos P, Masamune K, Tang G, Ren H and Tse Z T 2014 Intraoperative magnetic resonance imaging–conditional robotic devices for therapy and diagnosis *Proc. Inst. Mech. Eng.* H **228** 303
[224] Hata N, Moreira P and Fischer G 2018 Robotics in MRI-guided interventions *Top. Magn. Reson. Imaging* **27** 19
[225] Groenhuis V, Siepel F J, Welleweerd M K, Veltman J and Stramigioli S 2018 Sunram 5: An MR Safe Robotic System for Breast Biopsy *Proc. of The Hamlyn Symp. on Medical Robotics* (*London, United Kingdom*) pp 82–3
[226] Yakar D, Schouten M G, Bosboom D G, Barentsz J O, Scheenen T W and Fütterer J J 2011 Feasibility of a pneumatically actuated MR-compatible robot for transrectal prostate biopsy guidance *Radiology* **260** 241
[227] Krieger A *et al* 2011 An MRI-compatible robotic system with hybrid tracking for MRI-guided prostate intervention *IEEE Trans. Biomed. Eng.* **58** 3049
[228] Stoianovici D, Kim C, Petrisor D, Jun C, Lim S, Ball M W, Ross A, Macura K J and Allaf M E 2016 MR safe robot, FDA clearance, safety and feasibility of prostate biopsy clinical trial *IEEE/ASME Trans. Mechatronics* **22** 115
[229] Li G, Su H, Cole G A, Shang W, Harrington K, Camilo A, Pilitsis J G and Fischer G S 2014 Robotic system for MRI-guided stereotactic neurosurgery *IEEE Trans. Biomed. Eng.* **62** 1077
[230] Krueger Julia J *et al* 2006 Magnetic resonance imaging–guided balloon angioplasty of coarctation of the aorta *Circulation* **113** 1093
[231] Tzifa A *et al* 2010 Magnetic resonance-guided cardiac interventions using magnetic resonance-compatible devices: a preclinical study and first-in-man congenital interventions *Circ.: Cardiovascular Intervent.* **3** 585
[232] Ratnayaka K *et al* 2012 Real-time MRI-guided right heart catheterization in adults using passive catheters *Eur. Heart J.* **34** 380
[233] Mukherjee R K *et al* 2019 Evaluation of a real-time magnetic resonance imaging-guided electrophysiology system for structural and electrophysiological ventricular tachycardia substrate assessment *Europace* **21** 1432